Hindawi
Discrete Dynamics in Nature and Society
Volume 2023, Article ID 4403361, 27 pages
https://doi.org/10.1155/2023/4403361

Research Article

Blockchain-Based Inventory System considering Uncertain Carbon Footprints and Pandemic Effects

P. Mala,[1] **M. Palanivel**,[2] **and S. Priyan**[3]

[1]*National Engineering College, Kovilpatti, Tamil Nadu, India*
[2]*Mepco Schlenk Engineering College, Sivakasi, Tamil Nadu, India*
[3]*Amity University Tashkent, Tashkent, Uzbekistan*

Correspondence should be addressed to P. Mala; gurupmala@gmail.com

Received 1 September 2023; Revised 6 November 2023; Accepted 30 November 2023; Published 18 December 2023

Academic Editor: Mijanur Rahaman Seikh

The global supply chain has been severely impacted with the outbreak of COVID-19. The continuous supply of essential products in the post-COVID-19 world is a truly effective and strategic contest. The security and useability of inventory management are a main burden for industries along with the pressure from the government to fulfil the targets of net-zero economy in an uncertain circumstance. One of the most potential keys to these issues is an accurate demand forecasting process by blockchain technology. This article addresses a basic outline for blockchain-based supply chain (SC) and reveals how blockchain technology (BCT) can aid policymakers to cut carbon footprint during and postpandemic time in a fuzzy environment. This study fuzzifies all the carbon factors as intuitionistic triangular fuzzy numbers and uses a signed distance method to defuzzify the model. We consider that the retailer can embrace BCT to enhance demand forecasting. The planned scenario is modeled as an optimization problem to maximize the profit with low carbon emissions and suggest a solution method to solve it. A numerical example is also given to validate the model. We compare the optimal decisions of the SC with and without BCT. We discover that the pandemic and BCT have considerable influences on the optimal results. The study also shows that practitioners should exercise caution when developing operational strategies for maximizing profit with the least amount of carbon emissions during and postpandemic time.

1. Introduction

The crisis COVID-19 had a demonstrable effect on global supply chains (GSCs) in addition to several other harmful effects on human health, ecology, and the economy. The most obvious sign of pervasive strains in GSC is the extension of the supplier's delivery lead times across advanced economies from the end of 2020. The report stated according to Figure 1 that the supplier's delivery lead times have lengthened massively in recent months and that the extension is turning out to be longer than it was with the first COVID-19 shock [1]. Figure 1 also shows that there is a substantial quantity of divergency between advanced and emerging economies. Then, another study explored the pre- and post-COVID-19 effects on the logistics markets as the COVID-19 turns further into the past [2]. The graphic picture of the analysis is pictured in Figure 2. Even as we move toward a postpandemic situation, we are still seeing exceptional challenges in various GSC sectors such as demand forecast and transportation. For example, the current conflicts among nations (Russia-Ukraine, Israel-Hamas, etc.) have been causing massive devastation and human gloom just as the postpandemic recovery was picking up speed. A major interruption to the GSC and an energy crisis have accompanied the conflicts. The same worries about consumers and global transport sources that we encountered during the pandemic are sparked by these disruptive acts. This paper contends that in emergency pandemic scenarios such as COVID-19 and conflicts, the transit cost of GSC needs to be correlated with the intensity of the pandemic.

A new study reveals the extent of multinational companies' impact on climate change by estimating that a 1/5th of carbon emissions (CO_2) originate from the GSC of these firms [3]. Many industrialized nations set goals to cut CO_2

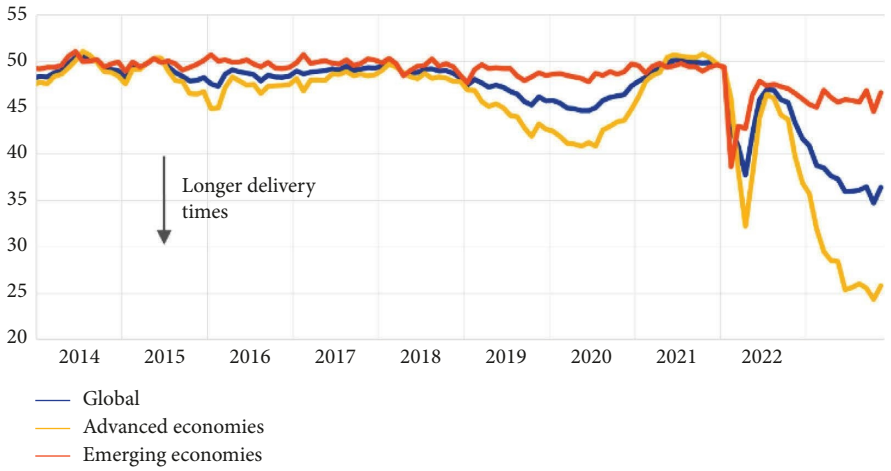

Figure 1: COVID-19 impact on worldwide suppliers' delivery times [1].

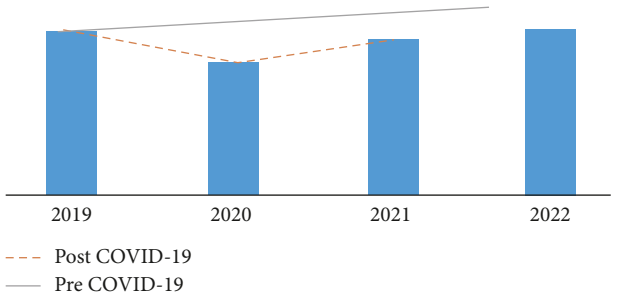

Figure 2: Analysis of the pre- and post-COVID-19 effects on the logistics markets [2].

and achieve net-zero by 2050 at the COP26 summit in Glasgow. However, we fell short of the goals in 2022, and if the current emissions intensity trends continue, the level of CO_2 will remain to rise and reach 62 GT by 2030. According to the World Emissions Clock [4], the estimate of CO_2 is based on an econometric vector autoregressive model of five sectors (industry, transport, energy, buildings, and agriculture and forestry) and 24 subsectors, across 180 economies. It is shown in Figure 3 and indicates that previous patterns are being followed without any modifications to strategies or other aspects. It demonstrates that overall world CO_2 is still increasing. The report also addressed the major sectors that make up the per capita CO_2 of the selected countries, and it is visualized in Figure 4. In addition to operational and technological energy efficacy measures to reduce the CO_2 intensity of all processes, a range of policies are required to support modal transitions to the least carbon-exhaustive SC policies to put GSC on the correct track for the net-zero scenario. Trade advisors feel that green technology might ease to lessen CO_2 due to SC activities such as production, setup, and storage. Hence, all delegates (leaders of various countries) in the COP27 summit held in November 2022 agreed to invest in green technology to cut CO_2 [5]. The most effective SC strategies for lowering CO_2 through green technology investments have also been determined by multiple studies. Sarkis [6] asserted that the postpandemic economic recovery would not disregard established standards and unease for the ecology. This work connects the impacts of pandemics and efforts to reduce CO_2 by green technology investment in GSC in the prepandemic situation.

One key issue with the works that have been published so far in the CO_2 area is that they assume the amount of CO_2 associated with various SC activities such as setup, production, storage, and transport are fixed known constants. In the real scenario, the amount of CO_2 is uncertain due to factors such as the state of the CO_2 filtration machine in the production firm, engine failure, quality of the raw material, nature of the fuel, or resources used. There may be fluctuations in the CO_2 parameters within specific ranges [7]. Hence, in line with Ruidas et al. [7], this study fuzzifies all the carbon factors as intuitionistic triangular fuzzy numbers.

Among the different fiscal issues faced by enterprises in the postpandemic, tightening acceptable financing has become more vital to retain operations and ensure business stability. A vital source of funding for small- and medium-sized firms is trade credit [8]. It still serves as an outlet for suppliers to provide credit to buyers, permitting them to postpone paying for accepted items and services. Even with the significance of trade credit in emergency situations, no studies link the effects of pandemics and trade credit financing in the postpandemic economy.

The intricacy of post-COVID-19 planning is much more multilayered and difficult than it was during the epidemic as time goes on. This is especially true for GSC members who have to predict customer expectations in the face of shifting markets and demand. There has never been more uncertainty about what to plan for and what data to use to achieve it. To manage the complexity and dangers in today's SCs, technology is essential. SC operations have been optimized by data analytics. An emerging trend known as Industry 4.0 is bringing industries into the next generation [9]. Among the cutting-edge technologies of Industry 4.0 is blockchain [10]. Blockchain technology (BCT) has a remarkable ability to handle large volumes of formless data in real time. It offers a single source of truth for supply and

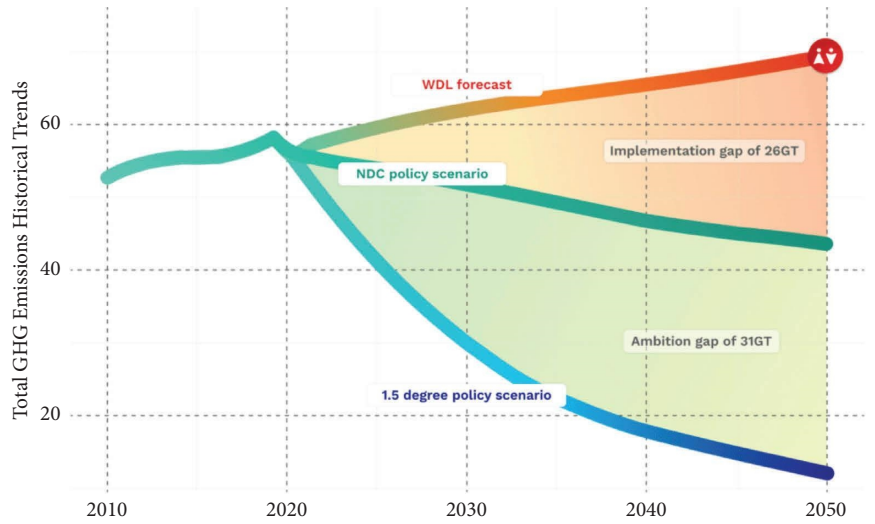

Figure 3: Estimation of CO_2 based on an econometric vector autoregressive model of five sectors [4]. Source: World Data Lab (World Emissions Clock).

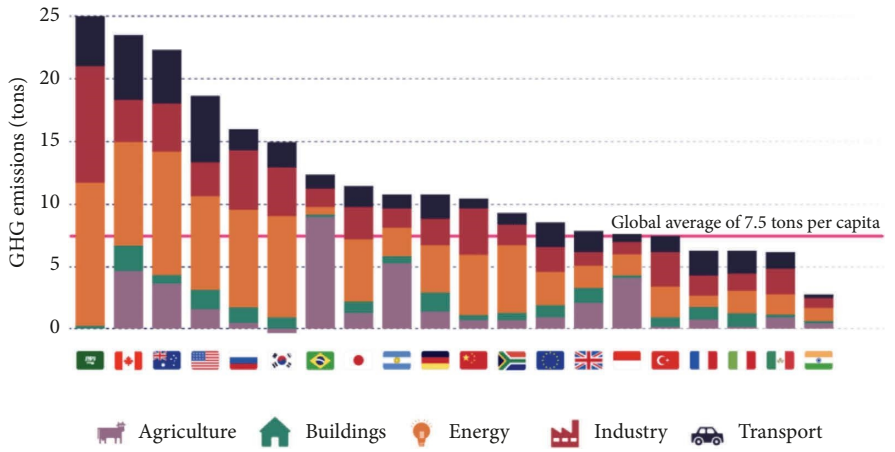

Figure 4: The per capita CO_2 of the selected countries broken down by major sectors [4]. Source: World Data Lab (World Emissions Clock).

demand data, which cuts errors, divergences, and disputes. That is, consumer demand forecasting based on BCT would expedite the process of making accurate decisions in the SC. Apart from the demand forecast, Suta and Tóth [11] stated that BCT can contribute to the efforts to cut CO_2 by steadily tracing CO_2 beliefs and aiding apparent and effective CO_2 swap. The blockchain-based inventory model has been shown to be one of the most critical aspects in cutting CO_2 in the SC.

We consider a GSC involving a supplier and a retailer under carbon taxation policy and multiperiod trade credit financing to control the shortage in an imperfect manufacturing system. The retailer remanufactures faulty items using his repair shop. The subsequent elements influence the operational decisions and coordination among the members of the SC: the pandemic effect, uncertain amount of carbon footprints, green technology investment, and application of blockchain technology. We examine these effects in this work by looking at the retailer's selling price, cycle time, amount of green investment and fraction of the cycle time with positive inventory-level decisions, and the demand forecasting problem of such a blockchain-based postpandemic GSC. We perform the analysis in three dimensions. First, we design the model by considering the practical influence of the COVID-19 pandemic on the transport sector in a crisp sense. Second, we adapt the model into a fuzzy sense. Third, we differentiate the analysis by taking blockchain technology into account. No study has looked at all three dimensions simultaneously to the best of our knowledge. We aimed to respond to the following three research questions in this paper:

(i) How should green technology investment be implemented to reduce CO_2 with the carbon taxation policy when CO_2 factors are uncertain?

(ii) How to handle and reuse the faulty items received from a foreign supplier to make efficient use of natural resources in emergency pandemic situations such as COVID-19 and conflicts?

(iii) How BCT changes decision-making in GSC?

(iv) What are the innovative solutions by applying BCT to deal with the logistics and customer demand worries during the pandemic and in comparable circumstances that arise in the future but are unpredictable?

To answer the above questions, we first investigate the optimization model for the integrated GSC with transport cost as proportional to COVID-19 intensity under the carbon taxation policy and trade credit finance, without considering fuzziness and blockchain. Then, we conduct a similar analysis by fuzzifying all the carbon factors as intuitionistic triangular fuzzy numbers into the model. We then examine both cases with and without BCT use. Last, we make a comparison of the optimal selling price, cycle time, fraction of the cycle time with a positive inventory level, green investment, and total profit of the GSC with and without applying BCT.

The remnant of the article is shaped as follows: In Section 2, we frame our study by spotting the research gap and reviewing the relevant literature. In Section 3, we introduce the notations and assumptions of the study. Section 4 constructs the model with the real effect of the pandemic on the transport sector and defuzzify the model by a signed distance method. In Section 5, we incorporate the BCT into the model and derive the main results of the study. We conduct numerical analysis to generate sensible insights from the analytical derivatives in Section 6. At the end, we draw the conclusion of the work and offer potential directions for future studies.

2. Literature Review

Our research is focused on four streams of the literature: (i) inventory management for imperfect production process in a supply chain, (ii) supply chain model with pandemic effects and trade credit finance, (iii) sustainable supply chain with CO_2 regulation and green investment, and (iv) application of BCT in the supply chain system.

2.1. Inventory Management for the Imperfect Production Process in a Supply Chain. Supply chain (SC) is the backbone of every business operation. It is seemingly more complicated and global, making it tough to keep track of inventory management. The ability to govern imperfect production processes is one of the aspects that affect SC's success, along with effective inventory management. Many production firms exhibit imperfection in their production processes due to numerous factors such as breakdowns in machinery, erratic power outages, worker and operator skill deficits, the quantity and quality of supplied raw materials, unexpected episodes in competitive markets, natural disasters, and pandemics [12]. The manufacturer would typically have a few options for handling this issue, such as rejecting and scrapping the faulty items, selling the salvaged items as new, or reworking the faulty items. In this case, the rework processes typically reduce the waste of the production company. Rework is raising areas of interest for scholars related to inventory management nowadays. In this context, a few researchers (see [12–20]) developed inventory models that considered imperfect production processes and rework policies. For instance, Al-Salamah [13] developed a production inventory model for a flawed production process with synchronous and asynchronous flexible rework rates. Lin et al. [14] designed inventory models for flawed items with an equal-sized supply policy under the hypothesis that the producer oversees production, inspection, and reworking processes. Jauhari and Wangsa [15] developed a closed-loop SC with green technology investment to cut CO_2 and take-back investment to raise the number of returned items amassed from the market by the manufacturer. Ali et al. [16] studied the optimal policy of a production firm based on production control, the greenness of the products, and the rework of faulty goods.

In this context, international trade has become extremely crucial for modern business. These days, a buyer buys goods from a global supplier, and these items could not be flawless due to some common causes such as cargo fork lifting, deficient binding, and faulty palletization. Now, it is not feasible to send these faulty items back to the supplier as they are located a thousand miles away. In most cases, the buyer sends these minor faulty items to a local repair store for rework and returns them. In this regard, unlike earlier studies, Dey et al. [17] derived a GSC where buyers use their repair shops to remanufacture faulty items under different CO_2 reduction strategies and multiperiod trade credit financing. Similarly, Harun [18] proposed alternate shipment policies compared for the GSC model with a stochastic exchange rate, CO_2, and flawed items. In this context, Ahmed et al. [20] explored the synergic effect of reworking for faulty items with the combination of multiperiod delay in payment and partial backordering in GSCs.

2.2. Supply Chain Model with Pandemic Effects and Trade Credit Finance. The COVID-19 pandemic constitutes a novel mega disruption with deadly ramifications that has significantly impacted GSC and intensified financial stresses in a variety of unified industries. Amid the numerous fiscal obstacles confronted by firms during the pandemic, acquiring enough financing has grown gradually crucial for preserving operations and ensuring SC continuity. Trade credit is an essential financing source. It is still used by suppliers to offer buyers an extension of credit, enabling them to postpone paying for collected products and services. Despite the significance of trade credit in emergency pandemic situations, no studies have considered the effects of the pandemic and trade credit financing simultaneously in the SC model. Conversely, several studies have considered the effects of the pandemic and trade credit financing independently ([21–27] for trade credit and [28–34] for pandemic effects). Specifically, Tiwari et al. [21] analyzed a green SC model for flawed products with a trade credit policy. They reduced the SC cost and made a contrast in various trade credit states. Mondal et al. [22] derived a model for decaying items and conferred the impact of trade credit on the total cost. Padiyar et al. [23] studied various circumstances under alternate trade credit schemes for a SC of

a nondecaying item. Mittal and Sarkar [24] formed a GSC model where the retailer offers a certain credit period to the client to pay in full.

In the pandemic context, Mashud et al. [28] investigated optimum inventory decisions for SC with considerations of product deterioration, time-dependent holding costs, price-dependent demands, and CO_2 under COVID-19 pandemic effects. They introduced a realistic transport cost that hinges on the rate of the COVID-19 outbreak. Priyamvada and Kumar [29] designed a dynamic optimal framework that allows businesses to allocate funds to marketing initiatives while upholding a sufficient standard of customer care during COVID-19. Valizadeh et al. [30] posed a solution for the vaccine SC to tackle the obstacles in the public immunization program considering the government and the system concern during COVID-19. Mashud et al. [31] studied a hybrid payment SC model for post-COVID-19 recovery taking price-sensitive customer demand, discounts, inflation, and conservation technology investment for noninstantaneously decaying items into account. Alkahtani et al. [32] derived a nonlinear SC t model with a controllable production rate in order to offer the trade company an economic advantage in terms of the optimum total cost of production and to address various scenarios such as COVID-19. Das et al. [33] proposed a recovery model employing two warehouse perishable inventory directives to assess the effects of SC disruptions during the COVID-19 lockdown. In contrast to others, Xie and Tian [34] studied the influence of the COVID-19 on the corporate trade credit policy.

2.3. Sustainable Supply Chain with CO_2 Regulation and Green Investment. Organizations are under growing pressure to take the environmental effects of their SC operations into account since SC generates around 60% of all CO_2 globally. Companies are therefore searching for methods to lower their carbon footprint to meet legal obligations and establish a reputation for corporate social responsibility. Increasing ecological alertness has provoked scholars in the field of inventory management to develop sustainable SC models that adapt for CO_2. The effect of CO_2 on inventory decisions has been greatly observed and linked to numerous key issues, including CO_2 legislation ([7, 35–40]), green investment ([41–50]), and other SC activities. Lu et al. [36] took into consideration a GSC that encompasses material supply, producer production and delivery, and retailer ordering and sales to provide a cross-border production-inventory model for decaying goods under various CO_2 policy mixtures. Asadkhani et al. [37] formed a SC model with extraction and package stock policies and executed various CO_2 policies to control CO_2. Jauhari et al. [38] used variable production rates and paid a hybrid production scheme to cut CO_2 and SC costs. The effect of carbon tax legislation on CO_2 and collaborative savings in a multiechelon SC was studied by Halat et al. [39]. They revealed that the planned rule might cut coalition expenses and lower rates of CO_2. Ahmad et al. [40] recently developed a green inventory model with conservation technology for decaying goods in a CO_2 tax regulation.

The goal of green technology is to protect the atmosphere, remedy ecological harm that has earlier been done, cut greenhouse gas CO_2, and conserve the natural resources. Green technology has also become a burgeoning industry that has attracted enormous amounts of investment capital. There are several methods to invest in green technology, including putting up solar panels and wind turbines and utilizing electric cars and biomass energy. The advantages of investing in green technology include operational efficiency, various cost savings, favorable ratings in the ecosystem, social and corporate governance, and other various government incentives [17]. Huang et al. [41] examined the possibility of investing in green technology to find an integrated policy with consideration of ecological and economic merits under various CO_2 laws. Jauhari [43] invented a mathematical model for a manufacturer-multiretailer system to optimize the inventory level and investments under a carbon tax policy. His study centered on how CO_2 and energy consumption affected SC activities. Ruidas et al. [44] explored the effects of a concurrent investment in greening invention and CO_2 decline technologies in a green production model where the various inventory cost and CO_2 factors are considered as interval valued. Priyan [45] addressed an effect of green investment to reduce CO_2 in a flawed system. Marchi and Zanoni [46] extended Huang et al.'s [41] model, which explored the effects of carbon rules and green technologies on the joined inventory system of a two-echelon SC with consideration of CO_2 during the processes of production, transport, and storage. Jauhari et al. [47] proposed pricing and green inventory decisions for a SC with green investment and carbon tax regulations under hybrid production and stochastic demand. Alsaedi et al. [50] studied the effects of learning and CO_2 on a green SC model for faulty items in fuzzy environments with shortage.

2.4. Application of BCT in the Supply Chain System. The intricacy of post-COVID planning is considerably more multifaceted and difficult than it was previously. This is particularly true for SC managers who are responsible for forecasting customer expectations in the face of shifting markets and demand. The inability of SC managers to make projections solely based on historical data presents one of the biggest obstacles to planning after two years of upheaval. They cannot disregard the preceding two years either. The pandemic has drastically altered consumer behavior, but no one anticipated how reopening would affect these habits. It has never been more difficult to plan and identify the data you need to do so. Keeping this in mind, scholars have studied SC inventory models with different demand nature (see [51–53]). For example, Jauhari [51] addressed a three-stage inventory production system with equal-sized deliveries. He assumed that the demand on the buyer's side is stochastic. Then, Ruidas et al. [52] formed a production inventory model with stock- and selling price-dependent demands and variable production rates in an interval environment. Priyamvada and Kumar [29] developed an efficient optimal model for retailers with selling price and efficiency of the investment-dependent demand. Ruidas

et al. [53] suggested pricing tactics in an interval-valued production inventory model for high-tech items under demand disruption and price revision.

Around the world, the epidemic upended people's lives, and livelihoods, requiring customers and businesses to adopt new digital habits. Rehabbed homemakers gave up long-standing shopping habits, sending e-commerce into overdrive, and condensing ten years of digital adoption into a few short days. Businesses swiftly changed course and innovated to find new methods to engage with potential customers in response to the digital-first economy. The development of a digital SC imposes the approval of a few technologies, such as artificial intelligence (AI), blockchain technology (BCT), cloud computing, data science, 5G, IoT, and digital twins. Blockchain technology is one of the key technologies, and it plays an important role in initiating GSC strategies. It is remarkably adept at processing massive amounts of unstructured data in real time. Organizations miss out on valuable insights that can enhance their SC resilience and efficacy when they ignore such data. BCT helps firms to generate more dependable and trustworthy plans and forecasts by allowing them to regularly verify the legitimacy, originality, and integrity of data [54]. Implementing blockchain in SC is graphically shown in Figure 5. Most of the available studies on BCT adoption are carried out using case, simulation, or empirical studies, for example, benefits and challenges of introducing BCT (Azzi et al., [55]), classification of BCT applications (Helo and Hao [56]), and simulation of BCT (Longo et al. [54]).

There are some works analytically investigating SC optimization considering BCT ([57–63]). Wei et al. [57] presented some analytical results on production and order dynamics in the context of a discrete time vendor-managed inventory (VMI) SC. Manupati et al. [58] proposed the use of BCT to address various production allocation issues in a multiechelon SC under the carbon taxation policy. Zhu et al. [59] initially attempted to study the impacts of BCT on market share, and they focused on whether the powerful brand owner in a dual-channel SC should adopt BCT. Li [60] presented a conceptual outline for blockchain-based SCs and illustrated how BCT may facilitate the realization of key innovations, including contract automation, a shared platform, end-to-end information exchange and traceability, real-time updates, and quick and efficient asset transfers. Xu et al. [61] derived integration of a platform-based SC in the marketplace or reselling mode considering cross-channel effects and BCT. They considered that the manufacturer can adopt BCT to improve demand forecasting. Modares et al. [62] derived a new VMI model by applying BCT and considering ecological issues. They looked at BCT for SC management by taking into consideration the most important BCT execution criteria for retailer selection and optimization. According to Allenbrand [63], a consortium BCT with smart contracts integrated might create an incentive structure that would make forecast-based coordination attractive. Table 1 presents research gaps in relation to the body of literature.

2.5. Research Gaps

(i) The enormous effects of green technology investment to reduce CO_2 on the functionality of GSC systems have been emphasized by research on inventory management with the carbon taxation policy. A significant gap in the literature is that it treats the quantity of emitted CO_2 throughout SC activities as a fixed constant (Dey et al. [17]). However, in the real scenario, these quantities may not be fixed due to various issues. There may be fluctuations in the parameters within specific ranges (Ruidas et al. [7]). To fill this main research gap, this study fuzzifies all the carbon factors as intuitionistic triangular fuzzy numbers in the GSC.

(ii) The regular GSC activities have been severely affected by the COVID-19 pandemic due to sudden and unplanned lockdowns. Even if the post-pandemic era is rapidly approaching, we are still seeing the effects of the pandemic in the transport and financial sectors due to geopolitical issues such as the current conflicts (Russia-Ukraine and Israel-Hamas) and rising tensions among nations. These rambunctious acts raise the same issues that we encountered during the epidemic about customers, global transportation, and financial sources. Decision-makers should reconfigure their SC in both sectors to ensure business continuity in the post-COVID-19 era. Despite the importance of trade credit financing in emergency pandemic situations, no studies have considered the effects of the pandemic and trade credit financing simultaneously in the GSC model. This study fills this gap.

(iii) Firms are having extraordinary difficulties predicting demand quickly based on changing client requirements and preferences as COVID-19 becomes the new normal. Introducing a smart SC is an essential for firms enabling their effectiveness in the market. Demand forecasting based on BCT will speed up the SC's decision-making process. This research uses demand forecasting based on BCT to increase GSC efficiency.

2.6. Contributions of This Study. The given model contributes to the existing literature by considering more realistic issues inspired by the GSC disruptions caused by the COVID-19 pandemic in a postpandemic world such as pandemic effects, trade credit financing, blockchain-based demand forecasting, green technology investment, flawed production and recovery processes, and transport disruption. The methodology that is being given has the potential to be utilized in relation to the COVID-19 pandemic, future conflicts, and other unforeseen events. The following are the principal contributions:

(i) The connection between pandemic effects and the demand forecasting process has been studied since the pandemic has significantly changed the consumption pattern and accelerated the shift toward

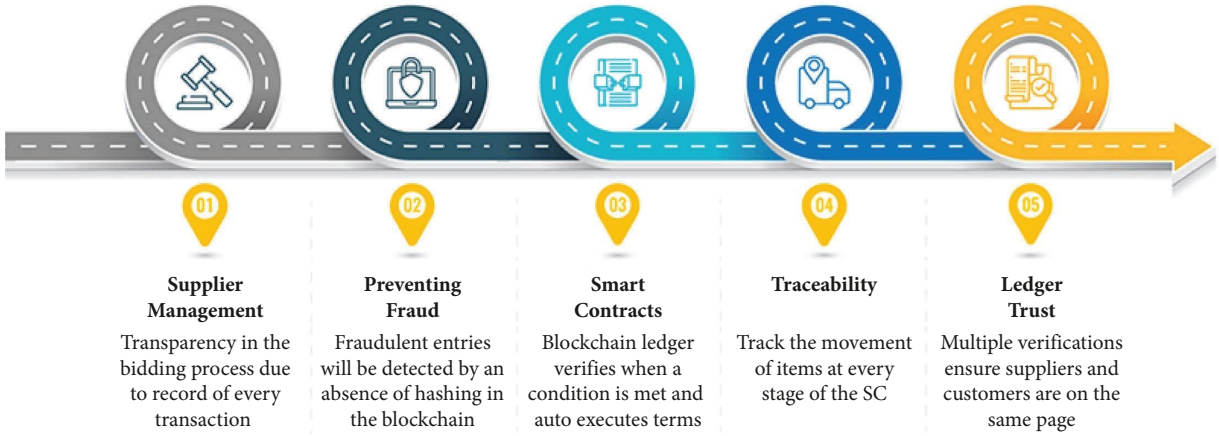

Figure 5: Implementing blockchain in SC.

more health and ecologically conscious and online purchases.

(ii) A convincing pandemic function is connected to the system's CO_2 to provide a clear image of the pandemic's effects on the transportation industry. One aspect of the pandemic function is the interaction between immune-compromised and diseased populations.

(iii) A GSC is formed under waste generation in terms of imperfect production and trade credit finance, where waste was generated during international trade and reworking is performed in the local repair shop of the retailer to avoid CO_2 due to transport activities.

(iv) An ecological fuzzy model based on blockchain technology is designed to control CO_2 via green technology investments in emergency pandemic situations.

2.7. Motivation and Objective. The COVID-19 pandemic has thrust many deficiencies in SC networks into the spotlight, particularly around visibility and integrity of customer demand and carbon footprint data. Many SC leaders have realized that their organizations are not prepared to handle major disruptions to their networks in the postpandemic world. However, this realization has begun to find the digitization of SCs by adopting emerging technologies such as blockchain that will allow firms to adapt to argue in real time. Blockchain technology plays a vital part in the digital transformation of SCs rising in a postpandemic world. The simple fact is BCT can effectively manage workflow across the entire SC and, through its strewn ledger approach, guarantee that data are accurate, transparent, and immutable critical capabilities in SC redesign. The focal essence of the study is to address a basic outline for blockchain-based GSC and reveal how BCT can help policymakers to cut CO_2 under uncertain postpandemic situations.

2.8. Research Methodology. Figure 6 provides a graphical illustration of the suggested methodology.

3. Notations and Assumptions

The following appropriate notations and assumptions are taken into consideration to formulate the mathematical model for the proposed realistic problem.

3.1. Notations. Parameters are as follows:

D_1 is the delay in first period payout (time unit)

C_t is the screening cost ($/unit)

O_c is the buyer's ordering cost ($/order)

r is the cost for the refund of faulty items ($/unit)

p is the cost for loss of goodwill ($/unit)

β is the proportion of delivered faulty items (%)

h_g is the holding cost for perfect items ($/unit per time unit)

y is the screening rate (unit)

η is the proportion of faulty items (%)

e_R is the emission due to the setup of the remanufacturing process (kg/setup)

e_r is the emission due to the repairing activities (kg/unit)

e_t is the emission due to the transportation actions (kg/unit)

e_h is the emission from holding inventories (kg/unit)

m_l is the markup fraction by a local store (%)

R_w is the reworking rate (unit/time time)

S_c is the setup cost of the rework shop ($/setup)

C_m is the cost of materials and labour to repair an item ($/unit)

h_l is the cost of holding items at a local store ($/unit per time unit)

T_A is the aggregate transport time of faulty items (time unit)

F is the fixed transport cost ($/trip)

C_i is the cost of shipping the faulty items ($/unit)

Table 1: Comparison of existing literature.

Author(s)	System type	Imperfect production process	Nature of CO_2 factors	Green technology investment	Trade credit financing	Pandemic effects	Blockchain technology
Zhang et al. [3]	GSC		Fixed				
Sarkis [6]	DSC		Fixed			✓	
Ruidas [7]	EPQ	✓	Interval				
Das et al. [12]	EPQ	✓	NA				
Al-Salamah [13]	EPQ	✓	NA				
Lin et al. [14]	EPQ	✓	NA				
Jauhari and Wangsa [15]	DSC	✓	Fixed	✓			
Ali et al. [16]	EPQ	✓	Fixed	✓			
Dey et al. [17]	GSC	✓	Fixed	✓	✓		
Harun [18]	GSC	✓	Fixed				
Priyan and Uthayakumar [19]	DSC	✓	NA				
Ahmed et al. [20]	GSC	✓	NA		✓		
Tiwari et al. [21]	EOQ		Fixed		✓		
Mondal et al. [22]	DSC	✓	Fixed		✓		
Padiyar et al. [23]	DSC	✓	NA		✓		
Mittal and Sarkar [24]	GSC		Fixed		✓		
Lin et al. [25]	DSC		NA		✓		
Kaushik [26]	EPQ		NA		✓		
Kumari et al. [27]	DSC		Fixed		✓		
Mashud et al. [28]	DSC		Fixed	✓		✓	
Valizadeh et al. [30]	DSC		NA			✓	
Mashud et al. [31]	DSC	✓	NA			✓	
Das et al. [33]	EPQ		NA			✓	
Xie and Tian [34]	EPQ		NA		✓	✓	
Priyan et al. [35]	DSC		Fixed				
Lu et al. [36]	GSC	✓	Fixed				
Priyan et al. [42]	EOQ	✓	Fixed	✓			
Jauhari [43]	DSC	✓	Fixed	✓			
Jauhari et al. [48]	DSC		Fixed	✓			
He [49]	EPQ		Fixed	✓			
Manupati et al. [58]	DSC		Fixed				✓
Zhu et al. [59]	DSC		NA				✓
Xu et al. [61]	DSC		Fixed				✓
Modares et al. [62]	DSC		Fixed				✓
This paper	GSC	✓	Fuzzy	✓	✓	✓	✓

GSC: global supply chain; DSC: domestic supply chain; NA: not applicable; EPQ: economic production quantity; EOQ: economic order quantity.

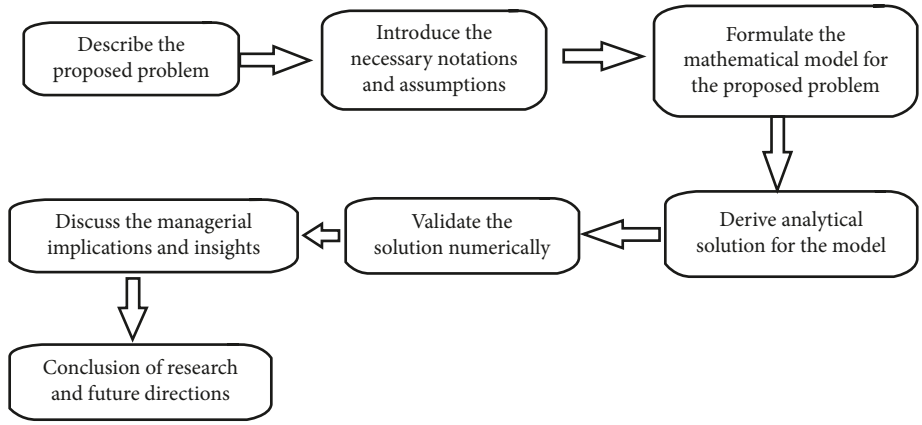

Figure 6: Diagram of the methodology.

C_1 is the carbon tax for unit carbon emissions (\$/unit)

α is the fraction of backordered demand (%)

C_l is the cost of lost sales (\$/unit per unit time)

γ is the backordering cost (\$/unit per time unit)

ζ is the size of the potential market

θ is the price sensitivity of sales price (\$)

ξ is the markup margin (%)

Q is the order quantity, dependent variable

$\sim$ is the fuzzy index

Decision variables are as follows:

ϑ_p is the sales price

G is the green investment amount

K is the fraction of the cycle time with a positive inventory level (%)

T is the cycle time (year)

3.2. Assumptions

(a) A single type of item is sent to the retailer by a global supplier, and each lot contains some faulty items. It is more expensive to send these faulty items to the supplier than to have them repaired in a local shop.

(b) The retailer gets an extra income from interest when the payment time (D_1) is longer than the cycle time (T). On the other hand, if D_1 is the accepted time and the cycle length K is lower, the buyer gets fewer interest but pays extra in opportunity costs (Dey et al. [17]).

(c) The inventory level remains positive for the K proportion of the cycle period. If η is the fraction of faulty items, then K has two portions: $K_1 = (1 - \eta)K$ and $K_2 = \eta K$. Here, K_1 and K_2 must lie within a [0, 1] interval (Dey et al. [17]).

(d) The vaccination has a 100% success rate. The initial vaccinated people must be less than the total people, i.e., $v_0 < P$. The infection rate κ lies in [0, 1], and the vaccination rate v_κ is positive, i.e., $v_\kappa > 0$. No one will be infected if there are no infected people (Mashud et al. [28]).

4. Model Formulation

A buyer will constantly try to sell the most consumer required items to their retail shop. The shop tried to pay as little as possible for the product the customer desired. Intercontinental trade is now extremely important for modern business in this setting. The things that a retailer now purchases from a global source might not be flawless due to freight fork lifting, inadequate packaging, false palletization, etc. Keeping this in mind, we investigate a global blockchain-based SC where retailers use their repair facilities to remanufacture defective goods while also considering the transport cost as a function of COVID-19 intensity. A trade credit is offered by the supplier to the retailer to make the payment in the emergency pandemic situation. We believe the retailer can embrace blockchain technology to enhance demand forecasting since lack of visibility into consumer behavior has made demand and supply unpredictable caused by the COVID-19 pandemic. We also assume that the uncertain amount of CO_2 is emitted due to various factors (Ruidas et al. [7]) during SC activities, and the system follows a carbon taxation policy to reduce CO_2 by investing in green technology. The considered scenario is modeled as an optimization problem to maximize the profit function while reducing CO_2 and suggest a solution method to solve it. In this context, we have developed two fuzzy mathematical models with and without applying blockchain technology.

4.1. Model without Applying Blockchain. In the proposed GSC system, the retailer orders products from a global supplier and sells them through the online channel to consumers at the retail price ϑ_p. Then, we consider the online demand to be $\lambda = (1 + \mu)\zeta - \theta\vartheta_p(1 + \xi) + \varepsilon$ where $\mu > 0$ is the retailer's power to grow the size of the prospective retail market and ε is a normal random variable with mean 0 and variance σ_0^2, which can be viewed as the demand noise. Here, we use δ to denote the private market signal that results from channel and user interaction, such as past sales data. Following Yu et al. [64], we state $\delta = \varepsilon + \eta$, where η is the instability of demand noise from distorted data and is a normal random variable with mean 0 and variance σ^2, which can be

viewed as the signal noise. The retailer detects the demand signal and shares it with the supplier. The detected signal for the demand noise follows the Bayesian rule, which is an unbiased estimator of ε, *i.e.*, $E[\delta|\varepsilon] = \varepsilon$. Then, we similarly have $E[\varepsilon|\delta] = (\sigma_0^2/\sigma^2 + \sigma_0^2)\delta = t\delta$ and Var $[\varepsilon + \delta] = t\sigma^2$, where $t = (\sigma_0^2/\sigma^2 + \sigma_0^2)$. This approach to the information structure is widely used in earlier research, and Vives [65] provides a detailed proof. We can rewrite $\varepsilon|\delta$ as $t\delta + \varepsilon^*$, where ε^* follows a normal random distribution with mean 0 and variance $t\sigma^2$.

Now, the demand function can be reexpressed as $\lambda = (1+\mu)\zeta - \theta\vartheta_p(1+\xi) + t\delta + \varepsilon^*$.

CO_2 originates from the warehousing operation (which stores both high-quality items), repairs, remanufacturing setup, and defective item shipping. Below is the formulation of the corresponding CO_2 process.

After screening, the η portion of items is found faulty as ηKTλ. Thus, CO_2 associated with the repairs is given as $e_r\eta$KTλ. Shipment of faulty items ηKTλ emits CO_2, which is calculated by $e_t\eta$KTλ, where e_t is the amount of CO_2 generated per unit item.

The warehouse, where both perfect and imperfect items are kept, releases certain emissions. Consequently, the amount of CO_2 released during storage is given as $e_h[((1-\eta)^2K^2T\lambda/2) + (\eta T(K\lambda)^2/y)]$.

Hence, total CO_2 emitted during SC activities is $e_R + e_r\eta$KT$\lambda + e_t\eta$KT$\lambda + e_h(((1-\eta)^2K^2T\lambda/2) + (\eta T(K\lambda)^2/y))$.

The SC members intend to invest in green technologies to transition to a more environmentally friendly industrial system. Green chemistry (biodegradable polymers and green chemical processes), renewable energy (solar, wind, and hydro), and technology that makes recycling easier are a few examples of the various types of green technology (100% recycled tin, precious metals). A well-known example of green technology is the solar cell. We consider the amount of carbon reduction investment function $R(G) = \pi(1 - e^{-mG})$ (Dey et al. [28]), where m implies the efficacy of the technology used for reduction of CO_2. $R(G) \longrightarrow 0$ when $G \longrightarrow 0$ and $R(G) \longrightarrow \pi$ as $G \longrightarrow \infty$. The graphical visualization of the green investment function $R(G)$ with respect to the efficiency of the technology m is shown in Figure 7.

Now, as pointed out by Dey et al. [17], the total profit function of the entire GSC with the carbon taxation policy and trade credit finance in a crisp nature without pandemic effects is expressed as

$$\begin{aligned}\mathrm{TP}(T,K,G,\vartheta_p) = {} & \underbrace{\vartheta_p\lambda}_{\text{income from selling items}} + \underbrace{S_I\left(\lambda D_1 - \frac{T\lambda}{2}\right)}_{\text{interest income}} \\ & - \Bigg(\underbrace{\mathrm{HC}}_{\text{holding cost}} + \underbrace{\mathrm{CC}}_{\text{CO}_2\text{ cost}} + \underbrace{\frac{O_c}{T}}_{\text{ordering cost}} + \underbrace{C_tK\lambda}_{\text{inspection cost}} \\ & + \underbrace{\mathrm{CR}}_{\text{rework cost}} + \underbrace{\mathrm{TC}}_{\text{transportation cost}} + \underbrace{\mathrm{SC}}_{\text{shortage cost}} + \underbrace{(r+p)\beta K\lambda}_{\text{penalty cost}} \Bigg),\end{aligned} \tag{1}$$

where

$$\begin{aligned}\mathrm{HC} &= h_g\left[\frac{(1-\eta)^2K^2T\lambda}{2} + \frac{\eta T(K\lambda)^2}{y}\right], \\ \mathrm{CC} &= C_1\left[e_R + e_r\eta\mathrm{KT}\lambda + e_t\eta\mathrm{KT}\lambda + e_h\left(\frac{(1-\eta)^2K^2T\lambda}{2} + \frac{\eta T(K\lambda)^2}{y}\right)\right]\left(1 - \pi\left(1 - e^{-mG}\right)\right), \\ \mathrm{CR} &= (1+m_l)\left[\frac{S_c}{\eta\mathrm{KT}\lambda} + C_m + h_l\left(\frac{\eta\mathrm{KT}\lambda}{R_w} + T_A\right)\right], \\ \mathrm{TC} &= 2(1+m_l)\left(\frac{F}{\eta\mathrm{KT}\lambda} + C_i\right), \\ \mathrm{SC} &= \gamma\frac{\alpha\eta^2K^2T\lambda}{2} + \gamma\frac{\alpha(1-K)^2T\lambda}{2} + C_l(1-\alpha)(1-K_1)\lambda.\end{aligned} \tag{2}$$

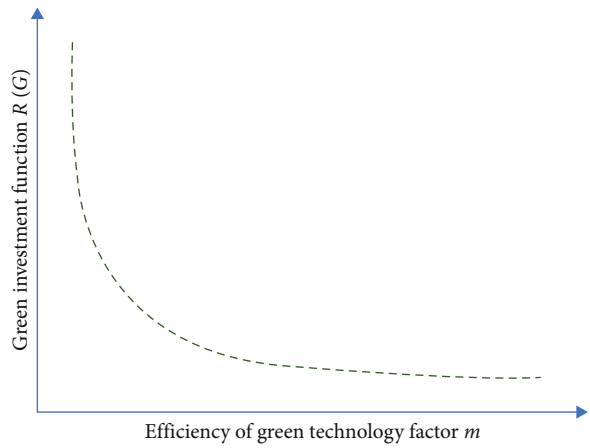

Figure 7: Graphical visualization of $R(G)$ against m.

However, many areas are still partially or entirely locked down because of COVID-19 spreading across the world. The scenario increases the cost of transportation. This study considers the scenario where the outcome is dependent on the pandemic's spread rate. There are totally P people in a town. These people are exposed to COVID-19 at an infection rate of κ. Nevertheless, the inoculation process is still ongoing; the acceleration rate is v_κ. Then, like Mashud et al. [28], the derived COVID function $I_p(t)$ with the initial infected people κ_0 and the initial vaccinated people v_0 is stated as

$$I_p(t) = \frac{\kappa_0 e^{\kappa t} P(P - v_0)}{P(P - v_0) + \left(v_\kappa t^3 + P\right)\left(\kappa_0 e^{\kappa t} - \kappa_0\right)}. \tag{3}$$

The standardized COVID-infected function $\varphi(T) = (I_p(T)/p)$ is expressed as

$$\varphi(T) = \frac{\kappa_0 e^{\kappa T}(P - v_0)}{P(P - v_0) + \left(v_\kappa T^3 + P\right)\left(\kappa_0 e^{\kappa T} - \kappa_0\right)}. \tag{4}$$

Taking the standardized COVID indicator function $\varphi(T)$ as an essential measure in mind, according to Mashud et al. [28], the transport cost rises $m_p\varphi$ times of the initial transport cost, i.e., $\mathrm{TC} = \mathrm{TC} \times (1 + m_p\varphi)$. At the apex of the COVID indicator function, this transport cost rises. Consequently, the transport cost can be remodified as

$$\mathrm{TC} = \left[2(1 + m_l)\left(\frac{F}{\eta \mathrm{K} \mathrm{T} \lambda} + C_i\right)\right]\left(1 + \frac{m_p \kappa_0 e^{\kappa T}(P - v_0)}{P(P - v_0) + \left(v_\kappa T^3 + P\right)\left(\kappa_0 e^{\kappa T} - \kappa_0\right)}\right). \tag{5}$$

It is observed from Figure 8 that in the real scenario, the amount of CO_2 is uncertain due to the state of the carbon-filtering equipment employed by the firm, general production technology, the caliber of the raw materials utilized, machine failure, the kind of fuels or energy used, etc. As a result, we consider that the CO_2 factors e_R (CO_2 emitted for setup of the repair store), e_r (CO_2 emitted for setup repair of one unit), e_t (CO_2 emitted for transport of defective items), and e_h (CO_2 emitted for holding) are all fuzzy, and we denote them here by the intuitionistic triangular fuzzy number as given below.

Intuitionistic fuzzy CO_2 emitted for setup of the repair shop $(\widetilde{e}_R)$ is $\left\{(\varphi_{e_R1}, \varphi_{e_R2}, \varphi_{e_R3}), (\varphi^I_{e_R1}, \varphi^I_{e_R2}, \varphi^I_{e_R3})\right\}$ where $\varphi^I_{e_R1} \le \varphi_{e_R1} \le \varphi_{e_R2} \le \varphi_{e_R3} \le \varphi^I_{e_R3}$.

Intuitionistic fuzzy CO_2 emitted for setup repair of one unit $(\widetilde{e}_r)$ is $\left\{(\varphi_{e_r1}, \varphi_{e_r2}, \varphi_{e_r3}), (\varphi^I_{e_r1}, \varphi^I_{e_r2}, \varphi^I_{e_r3})\right\}$ where $\varphi^I_{e_r1} \le \varphi_{e_r1} \le \varphi_{e_r2} \le \varphi_{e_r3} \le \varphi^I_{e_r3}$.

Intuitionistic fuzzy CO_2 emitted for transport of the defective item $(\widetilde{e}_t)$ is $\left\{(\varphi_{e_t1}, \varphi_{e_t2}, \varphi_{e_t3}), (\varphi^I_{e_t1}, \varphi^I_{e_t2}, \varphi^I_{e_t3})\right\}$ where $\varphi^I_{e_t1} \le \varphi_{e_t1} \le \varphi_{t2} \le \varphi_{e_t3} \le \varphi^I_{e_t3}$.

Intuitionistic fuzzy CO_2 emitted for holding items $(\widetilde{e}_h)$ is $\left\{(\varphi_{e_h1}, \varphi_{e_h2}, \varphi_{e_h3}), (\varphi^I_{e_h1}, \varphi^I_{e_h2}, \varphi^I_{e_h3})\right\}$ where $\varphi^I_{e_h1} \le \varphi_{e_h1} \le \varphi_{e_h2} \le \varphi_{e_h3} \le \varphi^I_{h3}$.

The CO_2 factors e_R, e_r, e_t, e_h in equation (1) are intuitionistic fuzzified as derived above; we can obtain the total profit function $\widetilde{\mathrm{TP}}(T, K, G, \vartheta_p)$ in the intuitionistic fuzzy sense as

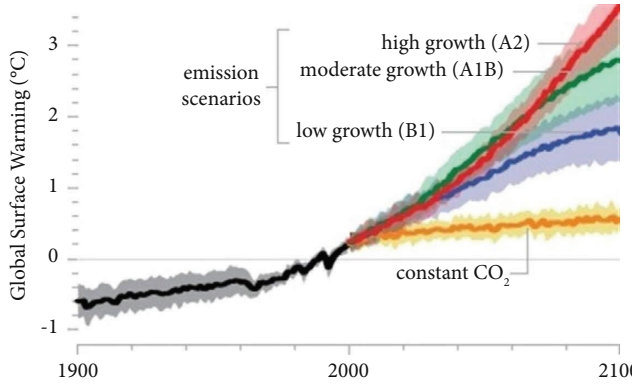

Figure 8: Uncertainty in climate science [66].

$$\begin{aligned}\widetilde{\mathrm{TP}}\left(T,K,G,\vartheta_p\right) &= \vartheta_p\lambda + S_I\left(\lambda D_1 - \frac{T\lambda}{2}\right) - h_g\left[\frac{(1-\eta)^2K^2T\lambda}{2} + \frac{\eta T(K\lambda)^2}{y}\right] - \frac{O_c}{T} - C_tK\lambda \\ &- \left[\widetilde{e}_R + \widetilde{e}_r\eta\mathrm{KT}\lambda + \widetilde{e}_t\eta\mathrm{KT}\lambda + \widetilde{e}_h\left(\frac{(1-\eta)^2K^2T\lambda}{2} + \frac{\eta T(K\lambda)^2}{y}\right)\right]\left(1-\pi\left(1-e^{-\mathrm{mG}}\right)\right) \\ &- C_tK\lambda - (1+m_l)\left[\frac{S_c}{\eta\mathrm{KT}\lambda} + C_m + h_l\left(\frac{\eta\mathrm{KT}\lambda}{R_w} + T_A\right)\right] \\ &- \left[2(1+m_l)\left(\frac{F}{\eta\mathrm{KT}\lambda} + C_i\right)\right]\left(1 + \frac{m_p\kappa_0e^{\kappa\mathrm{T}}(P-v_0)}{P(P-v_0) + \left(v_\kappa T^3 + P\right)\left(\kappa_0e^{\kappa\mathrm{T}} - \kappa_0\right)}\right) \\ &- \gamma\frac{\alpha\eta^2K^2T\lambda}{2} + \gamma\frac{\alpha(1-K)^2T\lambda}{2} + C_l(1-\alpha)(1-K_1)\lambda - (r+p)\beta K\lambda.\end{aligned} \tag{6}$$

When the CO_2 factors e_R, e_r, e_t, and e_h are described with the intuitionistic triangular fuzzy number, by using the signed distance method, the defuzzified values of $\widetilde{e}_R, \widetilde{e}_r, \widetilde{e}_t$, and $\widetilde{e}_h$ are given by

$$\begin{aligned}d_0\left(\widetilde{e}_R,\widetilde{0}\right) &= \frac{1}{8}\left(\varphi^I_{e_R1} + \varphi_{e_R1} + 4\varphi_{e_R2} + \varphi_{e_R3} + \varphi^I_{e_R3}\right), \\ d_0\left(\widetilde{e}_r,\widetilde{0}\right) &= \frac{1}{8}\left(\varphi^I_{e_r1} + \varphi_{e_r1} + 4\varphi_{e_r2} + \varphi_{e_r3} + \varphi^I_{e_r3}\right), \\ d_0\left(\widetilde{e}_t,\widetilde{0}\right) &= \frac{1}{8}\left(\varphi^I_{e_t1} + \varphi_{e_t1} + 4\varphi_{e_t2} + \varphi_{e_t3} + \varphi^I_{e_t3}\right), \\ d_0\left(\widetilde{e}_h,\widetilde{0}\right) &= \frac{1}{8}\left(\varphi^I_{e_h1} + \varphi_{e_h1} + 4\varphi_{e_h2} + \varphi_{e_h3} + \varphi^I_{e_h3}\right).\end{aligned} \tag{7}$$

Similarly, based on the above-defuzzified values, the defuzzified total profit function of the model $\widetilde{\mathrm{TC}}(T, K, G, \vartheta_p)$ (equation (6)) is obtained as

$$\begin{aligned} d_0\left(\widetilde{\mathrm{TP}}\left(T, K, G, \vartheta_p\right), \widetilde{0}\right) = {} & \vartheta_p\lambda + S_I\left(\lambda D_1 - \frac{T\lambda}{2}\right) - h_g\left[\frac{(1-\eta)^2K^2T\lambda}{2} + \frac{\eta T(K\lambda)^2}{y}\right] - \frac{O_c}{T} - C_tK\lambda \\ & - \eta K\lambda(1+m_l)\left[\frac{S_c}{\eta \mathrm{KT}\lambda} + C_m + h_l\left(\frac{\eta \mathrm{KT}\lambda}{R_w} + T_A\right)\right] \\ & - C_1\left[d_0(\widetilde{e}_R, \widetilde{0}) + d_0(\widetilde{e}_r, \widetilde{0})\eta \mathrm{KT}\lambda + d_0(\widetilde{e}_t, \widetilde{0})\eta \mathrm{KT}\lambda + d_0(\widetilde{e}_h, \widetilde{0})\left(\frac{(1-\eta)^2K^2T\lambda}{2} + \frac{\eta T(K\lambda)^2}{y}\right)\right]\left(1 - \pi\left(1 - e^{-\mathrm{mG}}\right)\right) + G \\ & - \left[2(1+m_l)\left(\frac{F}{\eta \mathrm{KT}\lambda} + C_i\right)\right]\left(1 + \frac{m_p\kappa_0 e^{\kappa \mathrm{T}}(P - v_0)}{P(P-v_0) + \left(v_\kappa T^3 + P\right)\left(\kappa_0 e^{\kappa \mathrm{T}} - \kappa_0\right)}\right) \\ & - \gamma\frac{\alpha\eta^2K^2T\lambda}{2} - \gamma\frac{\alpha(1-K)^2T\lambda}{2} - C_l(1-\alpha)(1-K_1)\lambda - (r+p)\beta K\lambda. \end{aligned} \tag{8}$$

4.2. Model with Applying Blockchain. This subsection looks at how the retailer might use BCT to enhance demand forecasts. If a retailer decides to use blockchain, there will be fixed costs ψ_f associated with putting it up as well as variable costs ψ_c associated with each product when the system uploads its data to the blockchain. The reason for this situation is that implementing BCT entails a fixed cost where the retailer must purchase the mandatory equipment to afford digital authorization (Niu et al. [67]). In addition, implementing BCT entails a unit operation cost where the retailer must pay staff salaries for the BCT operations, a fee for the BCT operations, and other expenses (Wang et al. [68]).

We are aware that the key characteristic of BCT is that it is exceedingly difficult or expensive to change the data stored there. According to Babich and Hilary [69], blockchain can also deliver more precise data. It leads to data transparency on BCT and data reliability, which further improves forecast accuracy [68]. The blockchain's signal regarding demand change is more dependable because the data are trustworthy and cannot be modified unilaterally. So, the demand noise of the private market signal δ (*i.e.* σ^2) is lessened with the aid of blockchain, showing a better value for t. Please be aware that the demand without blockchain is $\lambda = (1+\mu)\zeta - \theta\vartheta_p(1+\xi) + t\delta + \varepsilon^*$. We now employ χ to reflect the rise in demand brought on by the adoption of BCT. It is obvious that $\chi > \delta t$. Please take note that this approach to capturing blockchain characteristics is realistic and that many experts in the field of operations management have used it to assess the effect of BCT in their research (Xu et al. [61] and Yu [64]). Based on actual practice, the approach used to develop our model not only directs actual adoption of blockchain but also enhances prior research on the use of blockchain in operation management. The research presented here yields some noteworthy new findings. Figure 9 depicts the proposed BCT model.

Now, the defuzzified total profit function of the model $d_0(\widetilde{\mathrm{TP}}(T, K, G), \widetilde{0})$ (stated in equation (8)) by applying BCT is obtained as

$$\begin{aligned} d_0\left(\widetilde{\mathrm{TP}}\left(T, K, G, \vartheta_p\right), \widetilde{0}\right)^{\mathrm{BCT}} = {} & \vartheta_p\lambda + S_I\left(\lambda D_1 - \frac{T\lambda}{2}\right) - h_g\left[\frac{(1-\eta)^2K^2T\lambda}{2} + \frac{\eta T(K\lambda)^2}{y}\right] - \frac{O_c}{T} - C_tK\lambda \\ & - \eta K\lambda(1+m_l)\left[\frac{S_c + 2F}{\eta \mathrm{KT}\lambda} + C_m + 2C_i + h_l\left(\frac{\eta \mathrm{KT}\lambda}{R_w} + T_A\right)\right] \\ & - C_1\left[d_0(\widetilde{e}_R, \widetilde{0}) + d_0(\widetilde{e}_r, \widetilde{0})\eta \mathrm{KT}\lambda + d_0(\widetilde{e}_t, \widetilde{0})\eta \mathrm{KT}\lambda + d_0(\widetilde{e}_h, \widetilde{0})\left(\frac{(1-\eta)^2K^2T\lambda}{2} + \frac{\eta T(K\lambda)^2}{y}\right)\right]\left(1 - \pi\left(1 - e^{-\mathrm{mG}}\right)\right) + G \\ & - \left(1 + \frac{m_p\kappa_0 e^{\kappa \mathrm{T}}(P - v_0)}{P(P-v_0) + \left(v_\kappa T^3 + P\right)\left(\kappa_0 e^{\kappa \mathrm{T}} - \kappa_0\right)}\right) - \gamma\frac{\alpha\eta^2K^2T\lambda}{2} \\ & + \gamma\frac{\alpha(1-K)^2T\lambda}{2} - C_l(1-\alpha)(1-K_1)\lambda - (r+p)\beta K\lambda - \psi_c\lambda - \psi_f, \end{aligned} \tag{9}$$

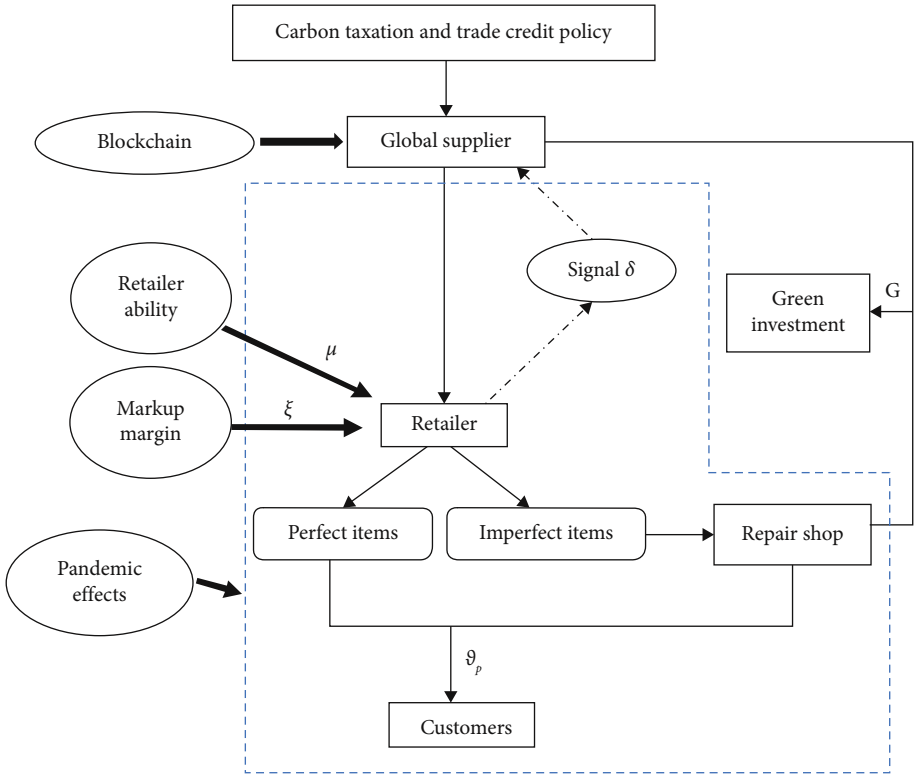

Figure 9: Proposed blockchain GSC system.

where $\lambda = (1+\mu)\zeta - \theta\vartheta_p(1+\xi) + \chi + \varepsilon^*$.

4.3. Model with the Cross-Channel Effect. In this case, the retailer sells goods through its own offline store where the retail price is hardly ever altered. There is often a base demand for this channel. In doing so, we can exactly capture the cross-channel effect as follows: The sales price of the offline channel is $\vartheta_{p'}$, and the corresponding demand is $\lambda_S = \lambda_0 + \tau\lambda$ where λ_0 is the base demand and τ captures the effect of online sales on offline demand, i.e., the cross-channel effect. Then, we formulate the profit of the system as follows:

$$
\begin{aligned}
d_0\left(\widetilde{\mathrm{TP}}\left(T,K,G,\vartheta_p\right),\tilde{0}\right)_S^{\mathrm{BCT}} = {} & \vartheta_{p'}\lambda_s + S_I\left(\lambda D_1 - \frac{T\lambda_s}{2}\right) - h_g\left[\frac{(1-\eta)^2K^2T\lambda_s}{2} + \frac{\eta T(K\lambda_s)^2}{y}\right] - \frac{O_c}{T} - C_tK\lambda_s \\
& - \eta K\lambda_s(1+m_l)\left[\frac{S_c+2F}{\eta \mathrm{KT}\lambda_s} + C_m + 2C_i + h_l\left(\frac{\eta \mathrm{KT}\lambda_s}{R_w} + T_A\right)\right] \\
& - C_1\left[d_0(\tilde{e}_R,\tilde{0}) + d_0(\tilde{e}_r,\tilde{0})\eta \mathrm{KT}\lambda_s + d_0(\tilde{e}_t,\tilde{0})\eta \mathrm{KT}\lambda_s + d_0(\tilde{e}_h,\tilde{0})\left(\frac{(1-\eta)^2K^2T\lambda_s}{2} + \frac{\eta T(K\lambda_s)^2}{y}\right)\right]\left(1-\pi\left(1-e^{-\mathrm{mG}}\right)\right) + G \\
& - \left(1 + \frac{m_p\kappa_0 e^{\kappa \mathrm{T}}(P-v_0)}{P(P-v_0) + \left(v_\kappa T^3 + P\right)\left(\kappa_0 e^{\kappa \mathrm{T}} - \kappa_0\right)}\right) - \gamma\frac{\alpha\eta^2K^2T\lambda_s}{2} \\
& + \gamma\frac{\alpha(1-K)^2T\lambda_s}{2} - C_l(1-\alpha)(1-K_1)\lambda_s - (r+p)\beta K\lambda_s - \psi_c\lambda_s - \psi_f.
\end{aligned}
\tag{10}
$$

5. Analytical Analysis for Optimality

The abovementioned problems (equations (8)–(10)) look to be nonlinear programming (NLP). We use the traditional calculus optimization approach to solve the proposed problem as derived in equation (9), and similarly, we can solve equations (8) and (10) as well. That is, it is essential to verify the necessary and sufficient conditions to determine the optimality of T, K, G, and ϑ_p:

$$\begin{aligned}\frac{\partial d_0\left(\widetilde{\mathrm{TP}}\left(T,K,G,\vartheta_p\right),\tilde{0}\right)^{\mathrm{BCT}}}{\partial T} &= \frac{O_c}{T^2}-\frac{S_I\lambda}{2}-h_g\left[\frac{(1-\eta)^2K^2\lambda}{2}+\frac{\eta(K\lambda)^2}{y}\right]\\ &-C_1\left[d_0\left(\tilde{e}_r,\tilde{0}\right)\eta K\lambda+d_0\left(\tilde{e}_t,\tilde{0}\right)\eta K\lambda+d_0\left(\tilde{e}_h,\tilde{0}\right)\left(\frac{(1-\eta)^2K^2\lambda}{2}+\frac{\eta(K\lambda)^2}{y}\right)\right]\left(1-\pi\left(1-e^{-\mathrm{mG}}\right)\right)\\ &-\eta K\lambda\left(1+m_l\right)\left[-\frac{S_c}{\eta KT^2\lambda}+h_l\left(\frac{\eta K\lambda}{R_w}\right)\right]-\gamma\frac{\alpha\eta^2K^2\lambda}{2}-\gamma\frac{\alpha(1-K)^2\lambda}{2}\\ &-2\left(1+m_l\right)\frac{F}{\eta\mathrm{KT}\lambda}\left(1+\frac{\Omega_1e^{\kappa\mathrm{T}}}{\kappa_0e^{\kappa\mathrm{T}}\left(\nu_\kappa T^3+P\right)-\kappa_0T^3\nu_\kappa+\Omega_2}\right)\\ &-2\left(1+m_l\right)C_i\left(1+\frac{\Omega_1e^{\kappa\mathrm{T}}\left(\kappa_0T^2\nu_\kappa\left(3-\kappa\mathrm{T}-3e^{\kappa\mathrm{T}}\right)\right)+\kappa\Omega_2}{P\left(P-\nu_0\right)+\left(\nu_\kappa T^3+P\right)\left(\kappa_0e^{\kappa\mathrm{T}}-\kappa_0\right)}\right)=0,\end{aligned}\tag{11}$$

where $\Omega_1=m_p\kappa_0\left(P-\nu_0\right)$ and $\Omega_2=P\left(P-\nu_\kappa\right)-\kappa_0P$

$$\begin{aligned}\frac{\partial d_0\left(\widetilde{\mathrm{TP}}\left(T,K,G,\vartheta_p\right),\tilde{0}\right)^{\mathrm{BCT}}}{\partial K} &= -h_g\left[\frac{(1-\eta)^2\mathrm{2KT}\lambda}{2}+\frac{\eta T2K\lambda^2}{y}\right]-C_t\lambda\\ &-C_1\left[d_0\left(\tilde{e}_r,\tilde{0}\right)\eta T\lambda+d_0\left(\tilde{e}_t,\tilde{0}\right)\eta T\lambda+d_0\left(\tilde{e}_h,\tilde{0}\right)\left(\frac{(1-\eta)^2\mathrm{2KT}\lambda}{2}+\frac{\eta T2K\lambda^2}{y}\right)\right]\left(1-\pi\left(1-e^{-\mathrm{mG}}\right)\right)\\ &-\eta\lambda\left(1+m_l\right)\left[\frac{S_c+2F}{\eta\mathrm{KT}\lambda}+C_m+h_l\left(\frac{\eta\mathrm{KT}\lambda}{R_w}+T_A\right)\right]-\eta\lambda\left(1+m_l\right)\left[-\frac{S_c}{\eta K^2T\lambda}+h_l\left(\frac{\eta\mathrm{KT}\lambda}{R_w}\right)\right]\\ &-\gamma\frac{2\alpha\eta^2\mathrm{KT}\lambda}{2}+\gamma\frac{2\alpha(1-K)T\lambda}{2}-C_l(1-\alpha)\lambda(-1+\eta)-(r+p)\beta\lambda\\ &+\left[2\left(1+m_l\right)\left(\frac{F}{\eta K^2T\lambda}\right)\right]\left(1+\frac{m_p\kappa_0e^{\kappa\mathrm{T}}\left(P-\nu_0\right)}{P\left(P-\nu_0\right)+\left(\nu_\kappa T^3+P\right)\left(\kappa_0e^{\kappa\mathrm{T}}-\kappa_0\right)}\right)=0,\end{aligned}\tag{12}$$

$$\begin{aligned}\frac{\partial d_0\left(\widetilde{\mathrm{TP}}\left(T,K,G,\vartheta_p\right),\tilde{0}\right)^{\mathrm{BCT}}}{\partial\vartheta_p} &= \left((1+\mu)\zeta+t\delta+\varepsilon^*\right)-2\theta\vartheta_p(1+\xi)+SI\theta(1+\xi)\left(D_1-\frac{T}{2}\right)\\ &-2h_g\theta(1+\xi)\left[\frac{\eta T(K)^2}{y}\right]\left((1+\mu)\zeta-\theta\vartheta_p(1+\xi)+t\delta+\varepsilon^*\right)+C_tK\theta(1+\xi)\\ &-h_g\theta(1+\xi)\frac{(1-\eta)^2K^2T}{2}+\theta(1+\xi)\Omega_3\left(1-\pi\left(1-e^{-\mathrm{mG}}\right)\right)\\ &+2\theta(1+\xi)\frac{\eta T(K)^2}{y}\left((1+\mu)\zeta-\theta\vartheta_p(1+\xi)+t\delta+\varepsilon^*\right)\left(1-\pi\left(1-e^{-\mathrm{mG}}\right)\right)\\ &+C_tK\theta(1+\xi)+\left(1+m_l\right)\left[\frac{S_c}{\eta\mathrm{KT}\theta^2(1+\xi)^2}+h_l\theta(1+\xi)\left(\frac{\eta\mathrm{KT}}{R_w}\right)\right]+\psi_c\theta(1+\xi)\\ &+\left[2\left(1+m_l\right)\left(\frac{F}{\eta\mathrm{KT}\theta^2(1+\xi)^2}\right)\right]\left(1+\frac{m_p\kappa_0e^{\kappa\mathrm{T}}\left(P-\nu_0\right)}{P\left(P-\nu_0\right)+\left(\nu_\kappa T^3+P\right)\left(\kappa_0e^{\kappa\mathrm{T}}-\kappa_0\right)}\right)\\ &+\gamma\frac{\alpha\eta^2K^2T\theta(1+\xi)}{2}-\gamma\frac{\alpha(1-K)^2T\theta(1+\xi)}{2}-C_l(1-\alpha)\left(1-K_1\right)\theta(1+\xi)\\ &+(r+p)\beta K\theta(1+\xi)=0,\end{aligned}\tag{13}$$

where
$\Omega_3 = d_0(\tilde{e}_r, \tilde{0})\eta \mathrm{KT} + d_0(\tilde{e}_t, \tilde{0})\eta \mathrm{KT} + d_0(\tilde{e}_h, \tilde{0})((1-\eta)^2 K^2 T/2)$

$$\frac{\partial d_0\left(\widetilde{\mathrm{TP}}\left(T, K, G, \vartheta_p\right), \tilde{0}\right)^{\mathrm{BCT}}}{\partial G} = \mathrm{C}_1\left[d_0(\tilde{e}_R, \tilde{0}) + d_0(\tilde{e}_r, \tilde{0})\eta \mathrm{KT}\lambda + d_0(\tilde{e}_t, \tilde{0})\eta \mathrm{KT}\lambda + d_0(\tilde{e}_h, \tilde{0})\left(\frac{(1-\eta)^2 K^2 T\lambda}{2} + \frac{\eta T(K\lambda)^2}{y}\right)\right]\pi \mathrm{me}^{-\mathrm{mG}} - 1 = 0. \tag{14}$$

Furthermore, Theorem 1 demonstrates the existence of second-order sufficient conditions.

Theorem 1. *The profit function $d_0(\widetilde{TP}(T, K, G, \vartheta_p), \tilde{0})^{BCT}$ is concave with respect to $T, K, G,$ and ϑ_p.*

Proof. See Appendix.

By solving equations (10)–(13), the optimal values of $T, K, G,$ and ϑ_p can be computed. The SC's total profit can be determined by inserting those optimum values in equation (9). Similarly, we shall prove the concavity of other two cases $d_0(\widetilde{\mathrm{TP}}(T, K, G, \vartheta_p), \tilde{0})$ and $d_0(\widetilde{\mathrm{TP}}(T, K, G, \vartheta_p), \tilde{0})_S^{\mathrm{BCT}}$ similar to Theorem 1. □

6. Numerical Analysis for Optimality

The proposed optimization model's effectiveness is numerically evaluated, and the outcomes of the existing model are utilized to improve decision-making. A GRG solver aids in the solution of the optimization model. This solver solution ensures that the Karush–Kuhn–Tucker requirements for local optimality have been met mathematically.

To illustrate the efficiency of our model, we consider Dey et al. [17] data. In addition, for the COVID-19 case, $p = 2000$, $\kappa = 0.4$, $v_\kappa = 0.6$, $\kappa_0 = 200$, $v_0 = 30\,0$, $m_p = 5$; for the fuzzy case, $\varphi^I_{e_R 1} = 3, \varphi_{e_R 1} = 5, \varphi_{e_R 2} = 7, \varphi_{e_R 3} = 8, \varphi^I_{e_R 3} = 9; \varphi^I_{e_r 1} = 2, \varphi_{e_r 1} = 3.5, \varphi_{e_r 2} = 5, \varphi_{e_r 3} = 6 \quad \varphi^I_{e_r 3} = 7; \quad \varphi^I_{e_t 1} = 3, \varphi_{e_t 1} = 5.5, \varphi_{e_t 2} = \quad 8, \varphi_{e_t 3} = 10, \varphi^I_{e_t 3} = 12; \varphi^I_{e_h 1} = 2.5, \varphi_{e_h 1} = \ 4, \varphi_{e_h 2} = 5.5, \varphi_{e_h 3} = 6.5, \varphi^I_{e_h 3} = 7.5$; and for the BCT case, $\mu = 0.04, \zeta = 500, \theta = 1.5, \xi = 0.2, \psi_c = 4, \psi_f = 1000, \chi = \ 60, \lambda_0 = 100, \delta = 10, t = 2$.

If industry adopted the carbon taxation policy under the COVID-19 effect and fuzzy environment, then the decision-maker can follow the proposed optimal strategy which is given in Table 2, and concavity of the profit function is graphically shown in Figure 10. The effects of the COVID-19 epidemic rate and vaccination on the total profit function are graphically depicted in Figures 11 and 12, respectively.

6.1. Discussion of Findings

(i) This study compares the retailer's profit with and without BCT in terms of retailer power (μ) and price sensitivity (θ). The values of each curve are obtained by deducting the retailer's profit without applying BCT from the one with applying BCT, i.e., changes in the retailer's profit after applying BCT. Without applying BCT, we set $\delta = 10$. With applying BCT, we set $\chi = 20,40,60$ respectively. Figure 13 reveals that if $\chi = 20$ then $\Pi^* \geq \Pi^{\mathrm{BCT}*}$ when $0 < \mu < 0.085$ and $\Pi^* < \Pi^{\mathrm{BCT}*}$ when $\mu > 0.085$. If $\delta = 40$ then $\Pi^* \geq \Pi^{\mathrm{BCT}*}$ when $0 < \mu < 0.063$ and $\Pi^* < \Pi^{\mathrm{BCT}*}$ when $\mu > 0.063$. If $\delta = 60$ then $\Pi^* \geq \Pi^{\mathrm{BCT}*}$ when $0 < \mu < 0.037$ and $\Pi^* < \Pi^{\mathrm{BCT}*}$ when $\mu > 0.037$. In reality, a lot of retailers take steps to strengthen their commercial power. If the retailer uses BCT, this behavior will therefore be advantageous to him.

(ii) Figure 14 shows that if $\chi = 20$ then $\Pi^* \geq \Pi^{\mathrm{BCT}*}$ when $0 < \theta < 3.5$ and $\Pi^* < \Pi^{\mathrm{BCT}*}$ when $\theta > 3.5$. If $\delta = 40$ then $\Pi^* \geq \Pi^{\mathrm{BCT}*}$ when $0 < \theta < 4.8$ and $\Pi^* < \Pi^{\mathrm{BCT}*}$ when $\theta > 4.8$. If $\delta = 60$ then $\Pi^* \geq \Pi^{\mathrm{BCT}*}$ when $0 < \theta < 5.7$ and $\Pi^* < \Pi^{\mathrm{BCT}*}$ when $\theta > 5.7$.

(iii) The table and graphs show the optimal strategies of GSC with and without blockchain technology when the system runs in an emergency pandemic situation such as COVID-19 and conflicts. The model by Dey et al. [17] derived similar GSC behaviors and proposed optimal strategies. It needs to be noted that Dey et al. [17] do not consider the effects of the pandemic, blockchain, and uncertainty. The current optimal strategies are more applicable than the Dey et al. [17] model since we considered all the realistic issues which are facing GSC currently.

(iv) From Table 1, the system considering BCT gives more profit than without BCT. That means the manager gets more profit by digitalizing the GSC system.

(v) The total profit drops off dramatically when the rate of the COVID-19 outbreak rises. Figure 12 illustrates how the SC's overall profits are affected by the rate of change of vaccine acceleration. With a rising rate of vaccine acceleration, the overall profit rises.

(vi) According to Figure 11, a rise in the COVID rate causes a noticeable increase in the effects of COVID-19 on the overall profit and cost. As can be observed from the chart, the higher rate of COVID has a substantial impact on transport costs, although other circumstances have allowed for a less sensitive change of the COVID effect. The effects of

the CO_2 cost are evident as well, and appropriate management of the CO_2 cost results in more profit.

(vii) Figure 15 reveals that CO_2 is less when we apply the BCT in the GSC system. It is not surprising because practically we know that CO_2 can automatically reduce when we use the online process instead of offline.

(viii) Figures 16 and 17 demonstrate the graphical visualization of profit function with associated cost.

(ix) In model 5, we consider that the retailer sells its products through its own offline store with the data $\tau = -0.3, \vartheta_{po} = 40$. The optimal solution of the special case is $T^* = 0.1422, K^* = 0.8457, G^* = 813.34, Q^* = 36812$ and $\Pi^{BCT*} = 30612023.12$. The outcome shows that the retailer's profit drops when it sells products through its offline channel. This result is relevant because storing physical items in the warehouse leads to substantial CO_2 and cost.

(x) Since every study has different findings, it is impossible to compare directly with earlier research. But if certain ideas are added or ignored, the current study converges with those studies. This analysis converges with Dey et al. [17], for instance, if the idea of the pandemic and uncertainty effects is disregarded, as well as the use of BCT.

(xi) In model 5, according to Figures 13 and 14, we conclude that (a) if the cross-channel effect is low (high), using BCT could result in more (less) CO_2. (b) Applying BCT increases profit for the GSC under high (low) platform power if the cross-channel effect is modest (high).

6.2. Managerial Insights. This paper offers the following managerial strategies that may be used in the global SC during and postpandemic to adapt to interruptions in transportation networks:

(i) In emergency pandemic situations, it is imperative to have knowledge of the transportation cost for each trip, as viewed from an industrial standpoint. With the use of this model, the store can quickly determine the cost of transportation and overall profit in any emergency.

(ii) The importance of the delay period cannot be overstated in trade credit finance. Players stand to gain greater profit if the delay time is extended.

(iii) The current economy places a great deal of importance on international trade, and as a result, SC management is critical to modern business. Due to a few factors, including shipping and repair or remanufacturing, the rate of CO_2 during worldwide trade significantly grows. Green technology can be used to manage CO2 properly, and managers must know how much to invest in cutting CO_2. Today, the international business enterprises, such as Intel, Google, Microsoft, and Apple, are currently adopting green technology. With the use of wind, solar, hydro, and biomass in the production of its goods, Intel is the industry leader in using renewable energy. Google is making changes to its processes to be more responsible and environmentally beneficial. It is still dedicated to achieving carbon neutrality and creating goods that support energy efficiency. Microsoft supports corporate ecoinitiatives using its own technologies. It also mentioned how its data centers would evolve, with a focus on research and development (R&D) for renewable energy and energy efficiency. Apple has committed to using entirely renewable energy to power its data centers, and it has encouraged the bulk of its suppliers to follow suit. The company has also set a target of producing no trash to save water and reduce CO_2. These companies might adopt operational strategies for maximizing profit with the least amount of CO_2 during and postpandemic time with the aid of the current study's policy recommendations.

(iv) Nowadays, the quantity of CO_2 is not fixed due to several issues. Therefore, decision-makers require expert knowledge to make the optimal strategy

Table 2: Result and contribution comparison with the previous study.

Decision variable	Model without applying BCT	Model with applying BCT
T^* (year)	0.0986	0.0991
K^* (%)	0.9651	0.9562
G^8 (%/cycle)	734.46	727.32
Q^* (units)	38231	37673
ϑ_p^* ($)	75.21	91.24
Π^{BCT*}/Π^* ($/cycle)	3015241.51	3104527.32

Note. Π^{BCT*}=min of $d_0(\widetilde{TP}(T, K, G, \vartheta_p), \widetilde{0})^{BCT}$ and Π^*=min of $d_0(\widetilde{TP}(T, K, G, \vartheta_p), \widetilde{0})$.

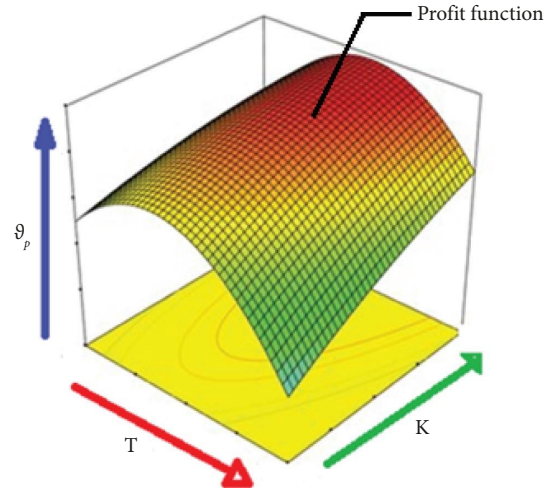

Figure 10: Concavity of the profit function.

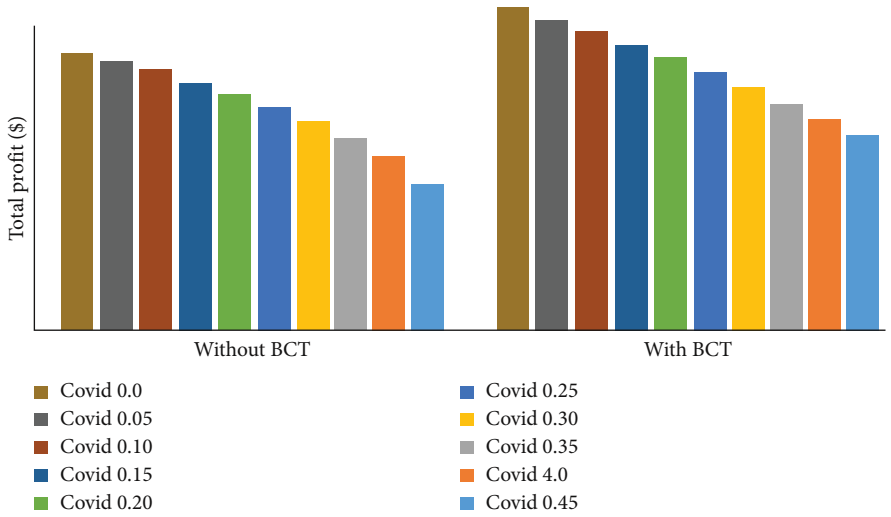

Figure 11: COVID-19 effect on total profit.

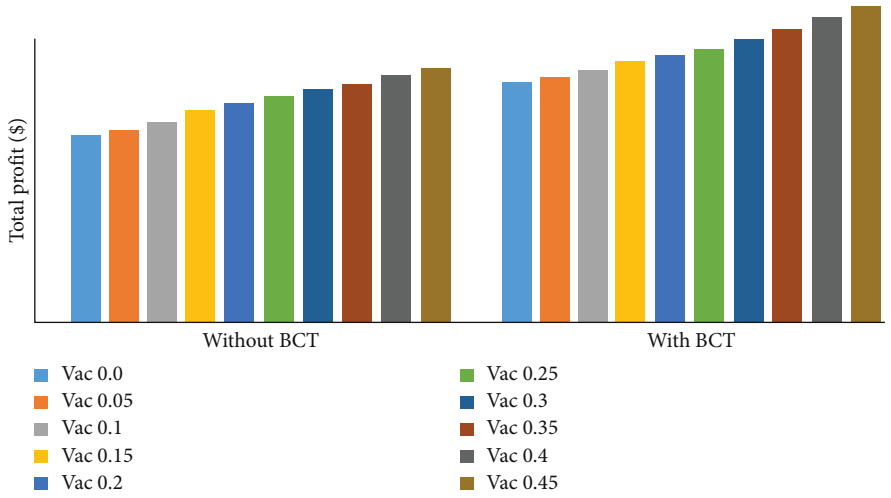

Figure 12: COVID-19 vaccination effect on total profit.

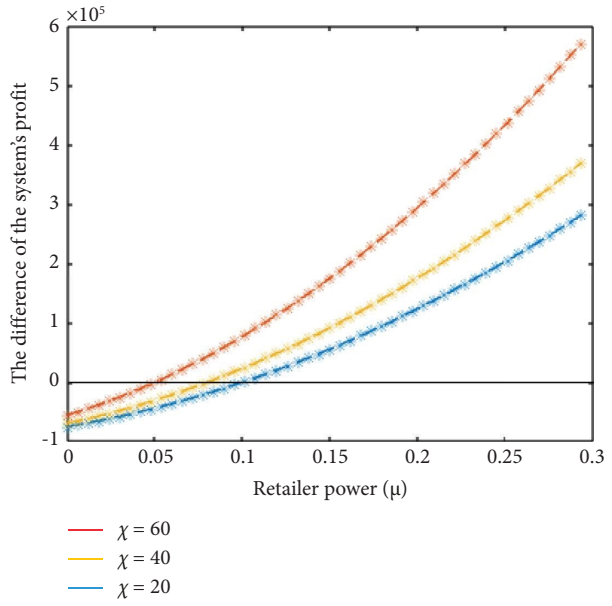

Figure 13: The difference in the system profits against μ with and without applying BCT.

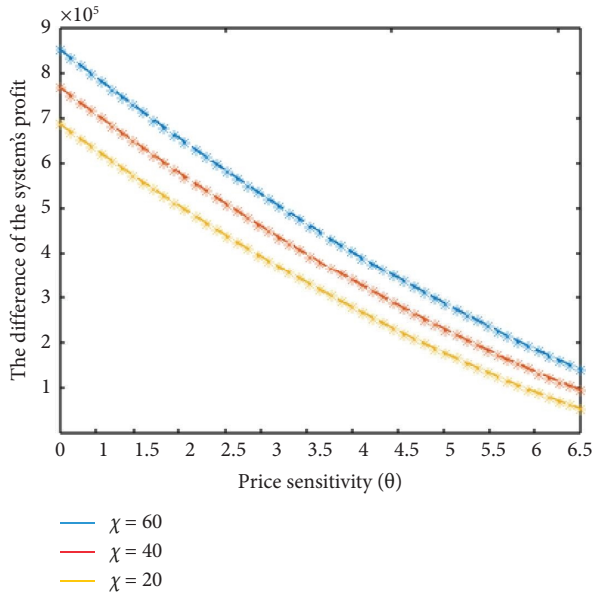

Figure 14: The difference in the system profits against θ with and without applying BCT.

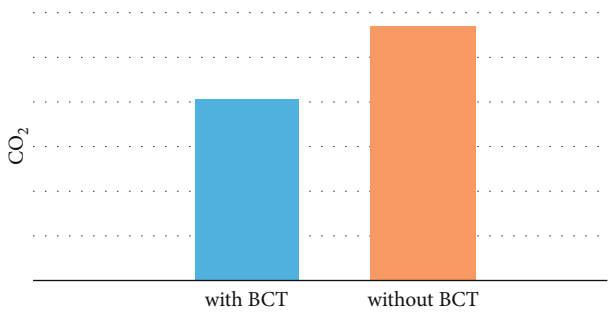

Figure 15: Total amount of CO_2 with and without BCT.

when the SC operates with an uncertain amount of CO_2. The policymakers of SC that operate with an uncertain amount of CO_2 can discover the appropriate optimal strategy by implementing this model.

(v) The study leads us to the conclusion that using BCT results in lower overall CO_2 and more profits for businesses in sectors with a pandemic effect and an uncertain amount of CO_2.

(vi) The utilization of BCT can enhance the lucid display of the product transportation routes from global suppliers to domestic customers via digital transactions. This would enable a re-evaluation of the GSC network's vulnerabilities and lower the risk of counterfeiting as well as the expense of correcting the harm.

(vii) Product acquisition and transport via the GSC are subject to strict observation. It is also feasible to maintain tabs on the stakeholders participating in the SC. BCT might be able to verify which stakeholder the product went through most recently if an issue is encountered during supply.

7. Conclusion

We study a blockchain-based GSC by incorporating pandemic effects and trade credit financing in an uncertain carbon footprint environment. We consider that retailers use their repair facilities to remanufacture defective goods and the transport cost as a function of COVID-19 intensity. Also, the retailer sells its products through its own online channel. The demand effect is exacerbated when basic forecasting techniques are used since the variation of the prediction inaccuracy is predicted to be greater than optimal. We take into consideration a demand forecasting process by BCT to address this problem. That is, the retailer can apply BCT to detect more market signals. This study fuzzifies all the carbon factors as intuitionistic triangular fuzzy numbers and uses a signed distance method to defuzzify the model. We initially study the basic model of the proposed problem without taking blockchain and fuzziness into account. We then investigate the mathematical model and the solution approach for the given problem with and without applying BCT by introducing fuzziness. Finally, we compare the optimal strategies with and without applying BCT. We observe that the pandemic and BCT have considerable impacts on the optimal decisions. The study also shows that the policymakers should be cautious in accounting uncertainty in the input carbon factors to develop operational strategies for maximizing profit at the lowest CO_2 during and postpandemic time.

Two major shortcomings of this study are that it does not account for selling price-dependent demand and no competition. This research can be expanded by considering selling price, customer service, and demand that is influenced by advertisements (Sarkar and Dey [70]). Another intriguing avenue for research is to include competition among multiple shops. Furthermore, as they are prevalent in practice, the inventory problem and product quality enhancement could be investigated. It is possible to examine the effects of further emerging technologies, such as artificial intelligence and big data, on supplier and retailer cooperation. This study can be expanded in the future by considering third-party logistics for the home delivery policy. A dynamic GSC system could be taken into consideration to take this research in a new direction.

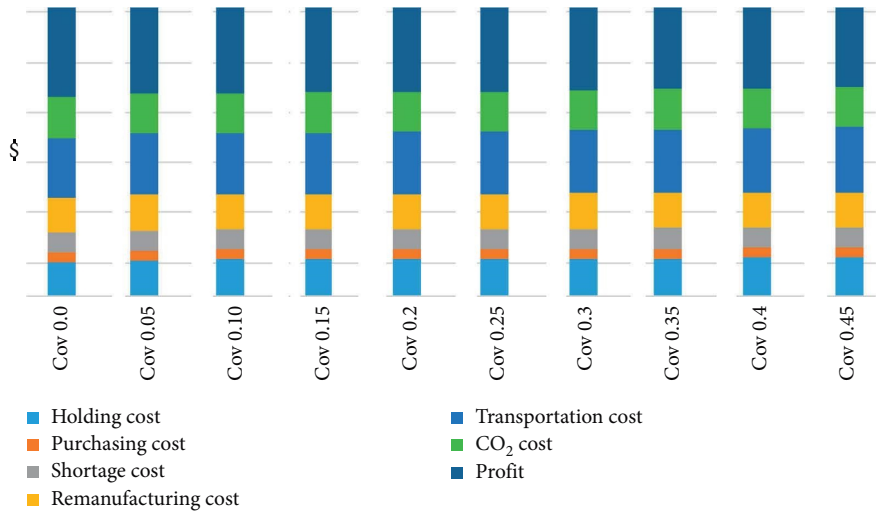

Figure 16: COVID-19 effect on profit and associated cost functions with BCT.

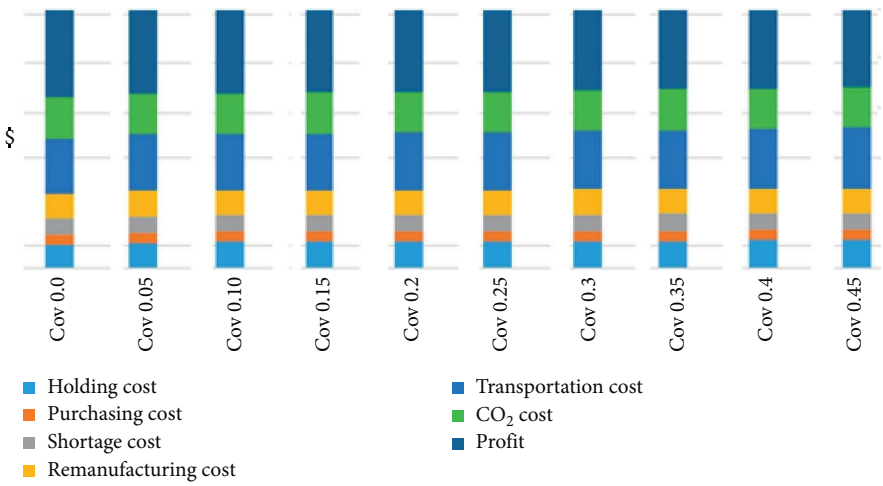

Figure 17: COVID-19 effect on profit and associated cost functions without BCT.

Appendix

A. First-Ordered Derivatives (Necessary Conditions)

$$
\begin{aligned}
\frac{\partial d_0\left(\widetilde{\mathrm{TP}}\left(T,K,G,\vartheta_p\right),\widetilde{0}\right)^{\mathrm{BCT}}}{\partial T} &= \frac{O_c}{T^2} - \frac{S_l\lambda}{2} - h_g\left[\frac{(1-\eta)^2K^2\lambda}{2} + \frac{\eta(K\lambda)^2}{y}\right] \\
&\quad - C_1\left[d_0(\widetilde{e}_r,\widetilde{0})\eta K\lambda + d_0(\widetilde{e}_t,\widetilde{0})\eta K\lambda + d_0(\widetilde{e}_h,\widetilde{0})\left(\frac{(1-\eta)^2K^2\lambda}{2} + \frac{\eta(K\lambda)^2}{y}\right)\right]\left(1-\pi\left(1-e^{-\mathrm{mG}}\right)\right) \\
&\quad - \eta K\lambda(1+m_l)\left[-\frac{S_c}{\eta KT^2\lambda} + h_l\left(\frac{\eta K\lambda}{R_w}\right)\right] - \gamma\frac{\alpha\eta^2K^2\lambda}{2} - \gamma\frac{\alpha(1-K)^2\lambda}{2} \\
&\quad - 2(1+m_l)\frac{F}{\eta\mathrm{KT}\lambda}\left(1+\frac{\Omega_1e^{\kappa\mathrm{T}}}{\kappa_0e^{\kappa\mathrm{T}}\left(\nu_\kappa T^3+P\right)-\kappa_0T^3\nu_\kappa+\Omega_2}\right) \\
&\quad - 2(1+m_l)C_i\left(1+\frac{\Omega_1e^{\kappa\mathrm{T}}\left(\kappa_0T^2\nu_\kappa\left(3-\kappa\mathrm{T}-3e^{\kappa\mathrm{T}}\right)\right)+\kappa\Omega_2}{P(P-\nu_0)+\left(\nu_\kappa T^3+P\right)\left(\kappa_0e^{\kappa\mathrm{T}}-\kappa_0\right)}\right), \\
\frac{\partial d_0\left(\widetilde{\mathrm{TP}}\left(T,K,G,\vartheta_p\right),\widetilde{0}\right)^{\mathrm{BCT}}}{\partial K} &= -h_g\left[\frac{(1-\eta)^2 2\mathrm{KT}\lambda}{2} + \frac{\eta T2K\lambda^2}{y}\right] - C_t\lambda \\
&\quad - C_1\left[d_0(\widetilde{e}_r,\widetilde{0})\eta T\lambda + d_0(\widetilde{e}_t,\widetilde{0})\eta T\lambda + d_0(\widetilde{e}_h,\widetilde{0})\left(\frac{(1-\eta)^2 2\mathrm{KT}\lambda}{2} + \frac{\eta T2K\lambda^2}{y}\right)\right]\left(1-\pi\left(1-e^{-\mathrm{mG}}\right)\right) \\
&\quad - \eta\lambda(1+m_l)\left[\frac{S_c+2F}{\eta\mathrm{KT}\lambda} + C_m + h_l\left(\frac{\eta\mathrm{KT}\lambda}{R_w} + T_A\right)\right] - \eta\lambda(1+m_l)\left[-\frac{S_c}{\eta K^2T\lambda} + h_l\left(\frac{\eta\mathrm{KT}\lambda}{R_w}\right)\right] \\
&\quad - \gamma\frac{2\alpha\eta^2\mathrm{KT}\lambda}{2} + \gamma\frac{2\alpha(1-K)T\lambda}{2} - C_l(1-\alpha)\lambda(-1+\eta) - (r+p)\beta\lambda \\
&\quad + \left[2(1+m_l)\left(\frac{F}{\eta K^2T\lambda}\right)\right]\left(1+\frac{m_p\kappa_0e^{\kappa\mathrm{T}}(P-\nu_0)}{P(P-\nu_0)+\left(\nu_\kappa T^3+P\right)\left(\kappa_0e^{\kappa\mathrm{T}}-\kappa_0\right)}\right), \\
\frac{\partial d_0\left(\widetilde{\mathrm{TP}}\left(T,K,G,\vartheta_p\right),\widetilde{0}\right)^{\mathrm{BCT}}}{\partial\vartheta_p} &= \left((1+\mu)\zeta + t\delta + \varepsilon^*\right) - 2\theta\vartheta_p(1+\xi) + SI\theta(1+\xi)\left(D_1 - \frac{T}{2}\right) \\
&\quad - 2h_g\theta(1+\xi)\left[\frac{\eta T(K)^2}{y}\right]\left((1+\mu)\zeta - \theta\vartheta_p(1+\xi) + t\delta + \varepsilon^*\right) + C_tK\theta(1+\xi) \\
&\quad - h_g\theta(1+\xi)\frac{(1-\eta)^2K^2T}{2} + \theta(1+\xi)C_1\Omega_3\left(1-\pi\left(1-e^{-\mathrm{mG}}\right)\right) \\
&\quad + 2\theta(1+\xi)\frac{\eta T(K)^2}{y}\left((1+\mu)\zeta - \theta\vartheta_p(1+\xi) + t\delta + \varepsilon^*\right)\left(1-\pi\left(1-e^{-\mathrm{mG}}\right)\right) \\
&\quad + (1+m_l)\left[\frac{S_c}{\eta\mathrm{KT}\theta^2(1+\xi)^2} + C_m + 2C_i + h_l\theta(1+\xi)\left(\frac{\eta\mathrm{KT}}{R_w} + T_A\right)\right] \\
&\quad + \left[2(1+m_l)\left(\frac{F}{\eta\mathrm{KT}\theta^2(1+\xi)^2}\right)\right]\left(1+\frac{m_p\kappa_0e^{\kappa\mathrm{T}}(P-\nu_0)}{P(P-\nu_0)+\left(\nu_\kappa T^3+P\right)\left(\kappa_0e^{\kappa\mathrm{T}}-\kappa_0\right)}\right) \\
&\quad + \gamma\frac{\alpha\eta^2K^2T\theta(1+\xi)}{2} - \gamma\frac{\alpha(1-K)^2T\theta(1+\xi)}{2} - C_l(1-\alpha)(1-K_1)\theta(1+\xi) \\
&\quad + (r+p)\beta K\theta(1+\xi) + \psi_c\theta(1+\xi) + C_tK\theta(1+\xi),
\end{aligned}
\tag{A.1}
$$

where
$\Omega_3 = d_0(\widetilde{e}_r, \widetilde{0})\eta\mathrm{KT} + d_0(\widetilde{e}_t, \widetilde{0})\eta\mathrm{KT} + d_0(\widetilde{e}_h, \widetilde{0})((1-\eta)^2 K^2 T/2)$

$$\frac{\partial d_0\left(\widetilde{\mathrm{TP}}\left(T,K,G,\vartheta_p\right),\widetilde{0}\right)^{\mathrm{BCT}}}{\partial G} = \mathrm{C}_1\left[d_0(\widetilde{e}_R,\widetilde{0}) + d_0(\widetilde{e}_r,\widetilde{0})\eta\mathrm{KT}\lambda + d_0(\widetilde{e}_t,\widetilde{0})\eta\mathrm{KT}\lambda + d_0(\widetilde{e}_h,\widetilde{0})\left(\frac{(1-\eta)^2K^2T\lambda}{2} + \frac{\eta T(K\lambda)^2}{y}\right)\right]\pi\mathrm{me}^{-\mathrm{mG}} - 1. \tag{A.2}$$

B. Sufficient Condition of Concavity

To prove the sufficient part for the classical optimization approach, it has to find the values of the principal minors of order 4×4; i.e., it has to calculate the values of the principal minors of the following Hessian matrix:

$$\det(H_{44}) = \det\begin{bmatrix} \frac{\partial^2 d_0\left(\widetilde{\mathrm{TP}}\left(T,K,G,\vartheta_p\right),\widetilde{0}\right)^{\mathrm{BCT}}}{\partial T^2} & \frac{\partial^2 d_0\left(\widetilde{\mathrm{TP}}\left(T,K,G,\vartheta_p\right),\widetilde{0}\right)^{\mathrm{BCT}}}{\partial T\partial K} & \frac{\partial^2 d_0\left(\widetilde{\mathrm{TP}}\left(T,K,G,\vartheta_p\right),\widetilde{0}\right)^{\mathrm{BCT}}}{\partial T\partial G} & \frac{\partial^2 d_0\left(\widetilde{\mathrm{TP}}\left(T,K,G,\vartheta_p\right),\widetilde{0}\right)^{\mathrm{BCT}}}{\partial T\partial \vartheta_p} \\ \frac{\partial^2 d_0\left(\widetilde{\mathrm{TP}}\left(T,K,G,\vartheta_p\right),\widetilde{0}\right)^{\mathrm{BCT}}}{\partial K\partial T} & \frac{\partial^2 d_0\left(\widetilde{\mathrm{TP}}\left(T,K,G,\vartheta_p\right),\widetilde{0}\right)^{\mathrm{BCT}}}{\partial K^2} & \frac{\partial^2 d_0\left(\widetilde{\mathrm{TP}}\left(T,K,G,\vartheta_p\right),\widetilde{0}\right)^{\mathrm{BCT}}}{\partial K\partial G} & \frac{\partial^2 d_0\left(\widetilde{\mathrm{TP}}\left(T,K,G,\vartheta_p\right),\widetilde{0}\right)^{\mathrm{BCT}}}{\partial K\partial \vartheta_p} \\ \frac{\partial^2 d_0\left(\widetilde{\mathrm{TP}}\left(T,K,G,\vartheta_p\right),\widetilde{0}\right)^{\mathrm{BCT}}}{\partial G\partial T} & \frac{\partial^2 d_0\left(\widetilde{\mathrm{TP}}\left(T,K,G,\vartheta_p\right),\widetilde{0}\right)^{\mathrm{BCT}}}{\partial G\partial K} & \frac{\partial^2 d_0\left(\widetilde{\mathrm{TP}}\left(T,K,G,\vartheta_p\right),\widetilde{0}\right)^{\mathrm{BCT}}}{\partial G^2} & \frac{\partial^2 d_0\left(\widetilde{\mathrm{TP}}\left(T,K,G,\vartheta_p\right),\widetilde{0}\right)^{\mathrm{BCT}}}{\partial G\partial \vartheta_p} \\ \frac{\partial^2 d_0\left(\widetilde{\mathrm{TP}}\left(T,K,G,\vartheta_p\right),\widetilde{0}\right)^{\mathrm{BCT}}}{\partial \vartheta_p\partial T} & \frac{\partial^2 d_0\left(\widetilde{\mathrm{TP}}\left(T,K,G,\vartheta_p\right),\widetilde{0}\right)^{\mathrm{BCT}}}{\partial \vartheta_p\partial K} & \frac{\partial^2 d_0\left(\widetilde{\mathrm{TP}}\left(T,K,G,\vartheta_p\right),\widetilde{0}\right)^{\mathrm{BCT}}}{\partial \vartheta_p\partial G} & \frac{\partial^2 d_0\left(\widetilde{\mathrm{TP}}\left(T,K,G,\vartheta_p\right),\widetilde{0}\right)^{\mathrm{BCT}}}{\partial \vartheta_p^{\,2}} \end{bmatrix}. \tag{B.1}$$

Now, it can be claimed that the profit function is concave, only when the values of the principal minors are alternate in sign.

Proof. For the optimal values of the decision variables, all principal minors of the Hessian matrices are alternate in sign. The detailed calculation along with second-ordered derivatives is provided as follows.

This section presents the Hessian computation for the optimality test and the derivative calculation:

$$\det(H_{44}) = \det\begin{bmatrix} \frac{\partial^2 d_0\left(\widetilde{\mathrm{TP}}\left(T,K,G,\vartheta_p\right),\tilde{0}\right)^{\mathrm{BCT}}}{\partial T^2} & \frac{\partial^2 d_0\left(\widetilde{\mathrm{TP}}\left(T,K,G,\vartheta_p\right),\tilde{0}\right)^{\mathrm{BCT}}}{\partial T\partial K} & \frac{\partial^2 d_0\left(\widetilde{\mathrm{TP}}\left(T,K,G,\vartheta_p\right),\tilde{0}\right)^{\mathrm{BCT}}}{\partial T\partial G} & \frac{\partial^2 d_0\left(\widetilde{\mathrm{TP}}\left(T,K,G,\vartheta_p\right),\tilde{0}\right)^{\mathrm{BCT}}}{\partial T\partial \vartheta_p} \\ \frac{\partial^2 d_0\left(\widetilde{\mathrm{TP}}\left(T,K,G,\vartheta_p\right),\tilde{0}\right)^{\mathrm{BCT}}}{\partial K\partial T} & \frac{\partial^2 d_0\left(\widetilde{\mathrm{TP}}\left(T,K,G,\vartheta_p\right),\tilde{0}\right)^{\mathrm{BCT}}}{\partial K^2} & \frac{\partial^2 d_0\left(\widetilde{\mathrm{TP}}\left(T,K,G,\vartheta_p\right),\tilde{0}\right)^{\mathrm{BCT}}}{\partial K\partial G} & \frac{\partial^2 d_0\left(\widetilde{\mathrm{TP}}\left(T,K,G,\vartheta_p\right),\tilde{0}\right)^{\mathrm{BCT}}}{\partial K\partial \vartheta_p} \\ \frac{\partial^2 d_0\left(\widetilde{\mathrm{TP}}\left(T,K,G,\vartheta_p\right),\tilde{0}\right)^{\mathrm{BCT}}}{\partial G\partial T} & \frac{\partial^2 d_0\left(\widetilde{\mathrm{TP}}\left(T,K,G,\vartheta_p\right),\tilde{0}\right)^{\mathrm{BCT}}}{\partial G\partial K} & \frac{\partial^2 d_0\left(\widetilde{\mathrm{TP}}\left(T,K,G,\vartheta_p\right),\tilde{0}\right)^{\mathrm{BCT}}}{\partial G^2} & \frac{\partial^2 d_0\left(\widetilde{\mathrm{TP}}\left(T,K,G,\vartheta_p\right),\tilde{0}\right)^{\mathrm{BCT}}}{\partial G\partial \vartheta_p} \\ \frac{\partial^2 d_0\left(\widetilde{\mathrm{TP}}\left(T,K,G,\vartheta_p\right),\tilde{0}\right)^{\mathrm{BCT}}}{\partial \vartheta_p\partial T} & \frac{\partial^2 d_0\left(\widetilde{\mathrm{TP}}\left(T,K,G,\vartheta_p\right),\tilde{0}\right)^{\mathrm{BCT}}}{\partial \vartheta_p\partial K} & \frac{\partial^2 d_0\left(\widetilde{\mathrm{TP}}\left(T,K,G,\vartheta_p\right),\tilde{0}\right)^{\mathrm{BCT}}}{\partial \vartheta_p\partial G} & \frac{\partial^2 d_0\left(\widetilde{\mathrm{TP}}\left(T,K,G,\vartheta_p\right),\tilde{0}\right)^{\mathrm{BCT}}}{\partial \vartheta_p{}^2} \end{bmatrix},$$

$$\begin{aligned}
\frac{\partial^2 d_0\left(\widetilde{\mathrm{TP}}\left(T,K,G,\vartheta_p\right),\tilde{0}\right)^{\mathrm{BCT}}}{\partial T^2} &= -\frac{2O_c}{T^3} - \eta K\lambda\left(1+m_l\right)\frac{2S_c}{\eta KT^3\lambda} \\
&\quad + 4\left(1+m_l\right)\frac{F}{\eta \mathrm{KT}^2\lambda} - 2\left(1+m_l\right)\frac{F}{\eta K\lambda}\left(\frac{4\Omega_1 e^{\kappa \mathrm{T}}\left(\nu_\kappa T^3 + P\kappa_0 e^{\kappa \mathrm{T}}\right) + \left(\nu_\kappa T^4 + P\right) - \kappa_0 T^4 \nu_\kappa}{\left(\kappa_0 e^{\kappa \mathrm{T}}\left(\nu_\kappa T^4 + P\right) - \kappa_0 T^4 \nu_\kappa + T\Omega_2\right)}\right) \\
&\quad - 2\left(1+m_l\right)\frac{F}{\eta K\lambda}\left(\frac{2\kappa_0 e^{\kappa \mathrm{T}}\left(\nu_\kappa T^2 + P\right) - 4\kappa_0 T^3 \nu_\kappa}{\left(2\kappa_0 T^4 \nu_\kappa + T\Omega_2\right)}\right)\left(\frac{2\Omega_1 e^{\kappa \mathrm{T}}\left(\nu_\kappa T^3 + P\kappa_0 e^{\kappa \mathrm{T}}\right)}{\left(4\kappa_0 e^{\kappa \mathrm{T}}\left(\nu_\kappa T^4 + P\right)\right)}\right) \\
&\quad - 2\left(1+m_l\right)C_i\left(\frac{\Omega_1 e^{\kappa \mathrm{T}}\left(\kappa_0 T^2 \nu_\kappa\left(3 - \kappa \mathrm{T} - 3e^{\kappa \mathrm{T}}\right)\right)}{P\left(P-\nu_0\right) + \left(\nu_\kappa T^3 + P\right)\left(\kappa_0 e^{\kappa \mathrm{T}} - \kappa_0\right)}\right) + \left(\frac{\kappa\Omega_2\Omega_1 e^{\kappa \mathrm{T}}}{\left(\nu_\kappa T^3 + P\right)\left(\kappa_0 e^{\kappa \mathrm{T}} - \kappa_0\right)}\right) < 0 \\
\frac{\partial^2 d_0\left(\widetilde{\mathrm{TP}}\left(T,K,G,\vartheta_p\right),\tilde{0}\right)^{\mathrm{BCT}}}{\partial K^2} &= -\left[\frac{(1-\eta)^2 2T\lambda}{2} + \frac{\eta T 2\lambda^2}{y}\right]\left(C_1 d_0\left(\tilde{e}_h,\tilde{0}\right)\left(1-\pi\left(1-e^{-\mathrm{mG}}\right)\right) + h_g\right) \\
&\quad - \frac{2Th_l\lambda^2\eta^2\left(1+m_l\right)}{R_w} - \lambda T\alpha\gamma\left(1+\eta^2\right) \\
&\quad - \left[4\left(1+m_l\right)\left(\frac{F}{\eta K^3 T\lambda}\right)\right]\left(1 + \frac{m_p\kappa_0 e^{\kappa \mathrm{T}}\left(P-\nu_0\right)}{P\left(P-\nu_0\right) + \left(\nu_\kappa T^3 + P\right)\left(\kappa_0 e^{\kappa \mathrm{T}} - \kappa_0\right)}\right) < 0 \\
\frac{\partial^2 d_0\left(\widetilde{\mathrm{TP}}\left(T,K,G,\vartheta_p\right),\tilde{0}\right)^{\mathrm{BCT}}}{\partial \vartheta_p^2} &= -2\theta\left(1+\xi\right) + S_l\theta\left(1+\xi\right)\left(D_1 - \frac{T}{2}\right) \\
&\quad - 2\theta^2\left(1+\xi\right)^2\frac{\eta T(K)^2}{y}\left(\left(1-\pi\left(1-e^{-\mathrm{mG}}\right)\right) - h_g\right) < 0 \\
\frac{\partial^2 d_0\left(\widetilde{\mathrm{TP}}\left(T,K,G,\vartheta_p\right),\tilde{0}\right)^{\mathrm{BCT}}}{\partial G^2} &= -\mathrm{C}_1\left[d_0\left(\tilde{e}_R,\tilde{0}\right) + d_0\left(\tilde{e}_r,\tilde{0}\right)\eta \mathrm{KT}\lambda + d_0\left(\tilde{e}_t,\tilde{0}\right)\eta \mathrm{KT}\lambda\right. \\
&\quad \left. + d_0\left(\tilde{e}_h,\tilde{0}\right)\left(\frac{(1-\eta)^2K^2T\lambda}{2} + \frac{\eta T(K\lambda)^2}{y}\right)\right]\pi m^2 e^{-\mathrm{mG}} < 0 \\
\frac{\partial^2 d_0\left(\widetilde{\mathrm{TP}}\left(T,K,G,\vartheta_p\right),\tilde{0}\right)^{\mathrm{BCT}}}{\partial T\partial K} &= \frac{\partial^2 d_0\left(\widetilde{\mathrm{TP}}\left(T,K,G,\vartheta_p\right),\tilde{0}\right)^{\mathrm{BCT}}}{\partial K\partial T} \\
&= -h_g\left[\frac{2(1-\eta)^2K\lambda}{2} + \frac{2\eta K\lambda^2}{y}\right] \\
&\quad - C_1\left[\left\{d_0\left(\tilde{e}_r,\tilde{0}\right) + d_0\left(\tilde{e}_t,\tilde{0}\right)\right\}\eta\lambda + d_0\left(\tilde{e}_h,\tilde{0}\right)\left(\frac{2(1-\eta)^2K\lambda}{2} + \frac{2\eta K\lambda^2}{y}\right)\right]\left(1-\pi\left(1-e^{-\mathrm{mG}}\right)\right) \\
&\quad - \eta\lambda\left(1+m_l\right)\left[\frac{S_c}{\eta K^2T^2\lambda} + h_l\left(\frac{\eta\lambda}{R_w}\right)\right] - \gamma\frac{2\alpha\eta^2K\lambda}{2} + \gamma\frac{2\alpha(1-K)\lambda}{2} \\
&\quad + 2\left(1+m_l\right)\frac{F}{\eta K^2T\lambda}\left(1 + \frac{\Omega_1 e^{\kappa \mathrm{T}}}{\kappa_0 e^{\kappa \mathrm{T}}\left(\nu_\kappa T^3 + P\right) - \kappa_0 T^3\nu_\kappa + \Omega_2}\right) \\
\frac{\partial^2 d_0\left(\widetilde{\mathrm{TP}}\left(T,K,G,\vartheta_p\right),\tilde{0}\right)^{\mathrm{BCT}}}{\partial T\partial G} &= \frac{\partial^2 d_0\left(\widetilde{\mathrm{TP}}\left(T,K,G,\vartheta_p\right),\tilde{0}\right)^{\mathrm{BCT}}}{\partial G\partial T} \\
&= -C_1\left[d_0\left(\tilde{e}_r,\tilde{0}\right)\eta K\lambda + d_0\left(\tilde{e}_t,\tilde{0}\right)\eta K\lambda + d_0\left(\tilde{e}_h,\tilde{0}\right)\left(\frac{(1-\eta)^2K^2\lambda}{2} + \frac{\eta(K\lambda)^2}{y}\right)\right]\left(-\pi \mathrm{me}^{-\mathrm{mG}}\right) \\
\frac{\partial^2 d_0\left(\widetilde{\mathrm{TP}}\left(T,K,G,\vartheta_p\right),\tilde{0}\right)^{\mathrm{BCT}}}{\partial T\partial \vartheta_p} &= \frac{\partial^2 d_0\left(\widetilde{\mathrm{TP}}\left(T,K,G,\vartheta_p\right),\tilde{0}\right)^{\mathrm{BCT}}}{\partial \vartheta_p\partial T} \\
&= -\frac{S_l\lambda'}{2} - h_g\left[\frac{(1-\eta)^2K^2\lambda'}{2} + \frac{\eta K^2 2\lambda\lambda'}{y}\right] \\
&\quad - C_1\left[d_0\left(\tilde{e}_r,\tilde{0}\right)\eta K\lambda' + d_0\left(\tilde{e}_t,\tilde{0}\right)\eta K\lambda' + d_0\left(\tilde{e}_h,\tilde{0}\right)\left(\frac{(1-\eta)^2K^2\lambda'}{2} + \frac{\eta K^2 2\lambda\lambda'}{y}\right)\right]\left(1-\pi\left(1-e^{-\mathrm{mG}}\right)\right) \\
&\quad - \eta K\lambda'\left(1+m_l\right)\left[\frac{S_c}{\eta \mathrm{KT}^2\lambda^2\lambda'} + h_l\left(\frac{\eta K\lambda'}{R_w}\right)\right] - \gamma\frac{\alpha\eta^2K^2\lambda'}{2} - \gamma\frac{\alpha(1-K)^2\lambda'}{2} \\
&\quad + 2\left(1+m_l\right)\frac{F}{\eta \mathrm{KT}\lambda^2\lambda'}\left(1 + \frac{\Omega_1 e^{\kappa \mathrm{T}}}{\kappa_0 e^{\kappa \mathrm{T}}\left(\nu_\kappa T^3 + P\right) - \kappa_0 T^3\nu_\kappa + \Omega_2}\right)
\end{aligned} \tag{B.2}$$

where $\lambda^{'} = -\theta(1+\xi)$.

$$
\begin{aligned}
\frac{\partial^2 d_0\left(\widetilde{\mathrm{TP}}\left(T,K,G,\vartheta_p\right),\widetilde{0}\right)^{\mathrm{BCT}}}{\partial K\partial G} &= \frac{\partial^2 d_0\left(\widetilde{\mathrm{TP}}\left(T,K,G,\vartheta_p\right),\widetilde{0}\right)^{\mathrm{BCT}}}{\partial G\partial K} \\
&= -C_1\left[d_0\left(\widetilde{e}_r,\widetilde{0}\right)\eta T\lambda + d_0\left(\widetilde{e}_t,\widetilde{0}\right)\eta T\lambda + d_0\left(\widetilde{e}_h,\widetilde{0}\right)\left(\frac{(1-\eta)^2 2\mathrm{KT}\lambda}{2} + \frac{\eta T2K\lambda^2}{y}\right)\right]\left(-\pi \mathrm{me}^{-\mathrm{mG}}\right), \\
\frac{\partial^2 d_0\left(\widetilde{\mathrm{TP}}\left(T,K,G,\vartheta_p\right),\widetilde{0}\right)^{\mathrm{BCT}}}{\partial K\partial \vartheta_p} &= \frac{\partial^2 d_0\left(\widetilde{\mathrm{TP}}\left(T,K,G,\vartheta_p\right),\widetilde{0}\right)^{\mathrm{BCT}}}{\partial \vartheta_p\partial K} \\
&= -h_g\left[\frac{(1-\eta)^2 2\mathrm{KT}\lambda^{'}}{2} + \frac{\eta T2K2\lambda\lambda^{'}}{y}\right] - C_t\lambda^{'} \\
&\quad - C_1\left[d_0\left(\widetilde{e}_r,\widetilde{0}\right)\eta T\lambda^{'} + d_0\left(\widetilde{e}_t,\widetilde{0}\right)\eta T\lambda^{'} + d_0\left(\widetilde{e}_h,\widetilde{0}\right)\left(\frac{(1-\eta)^2 2\mathrm{KT}\lambda^{'}}{2} + \frac{\eta T2K2\lambda\lambda^{'}}{y}\right)\right]\left(1-\pi\left(1-e^{-\mathrm{mG}}\right)\right) \\
&\quad - \eta\lambda^{'}\left(1+m_l\right)\left[\frac{S_c+2F}{\eta\mathrm{KT}\lambda} + C_m + h_l\left(\frac{\eta\mathrm{KT}\lambda}{R_w} + T_A\right)\right] + \eta\lambda\left(1+m_l\right)\frac{S_c+2F}{\eta\mathrm{KT}\lambda^2\lambda^{'}} \\
&\quad - \eta\lambda^{'}\left(1+m_l\right)\left[-\frac{S_c}{\eta K^2 T\lambda} + h_l\left(\frac{\eta\mathrm{KT}\lambda}{R_w}\right)\right] - \eta\lambda\left(1+m_l\right)\left[\frac{S_c}{\eta K^2 T\lambda^2\lambda^{'}} + h_l\left(\frac{\eta\mathrm{KT}\lambda^{'}}{R_w}\right)\right] \\
&\quad - \gamma\frac{2\alpha\eta^2\mathrm{KT}\lambda^{'}}{2} + \gamma\frac{2\alpha(1-K)T\lambda^{'}}{2} - C_l(1-\alpha)\lambda^{'}(-1+\eta) - (r+p)\beta\lambda^{'} \\
\text{where } \lambda^{'} &= -\theta(1+\xi) \\
&\quad + \left[2\left(1+m_l\right)\left(\frac{F}{\eta K^2 T\lambda}\right)\right]\left(1 + \frac{m_p\kappa_0 e^{\kappa\mathrm{T}}(P-\nu_0)}{P(P-\nu_0) + \left(\nu_\kappa T^3 + P\right)\left(\kappa_0 e^{\kappa\mathrm{T}} - \kappa_0\right)}\right) \\
\frac{\partial^2 d_0\left(\widetilde{\mathrm{TP}}\left(T,K,G,\vartheta_p\right),\widetilde{0}\right)^{\mathrm{BCT}}}{\partial G\partial \vartheta_p} &= \frac{\partial^2 d_0\left(\widetilde{\mathrm{TP}}\left(T,K,G,\vartheta_p\right),\widetilde{0}\right)^{\mathrm{BCT}}}{\partial G\partial \vartheta_p} \\
&= C_1\left[d_0\left(\widetilde{e}_r,\widetilde{0}\right)\eta\mathrm{KT}\lambda^{'} + d_0\left(\widetilde{e}_t,\widetilde{0}\right)\eta\mathrm{KT}\lambda^{'} + d_0\left(\widetilde{e}_h,\widetilde{0}\right)\left(\frac{(1-\eta)^2 K^2 T\lambda^{'}}{2} + \frac{\eta\mathrm{TK}^2 2\lambda\lambda^{'}}{y}\right)\right]\pi\mathrm{me}^{-\mathrm{mG}}.
\end{aligned}
\tag{B.3}
$$

Hence, the profit function $d_0\left(\widetilde{\mathrm{TP}}\left(T,K,G,\vartheta_p\right),\widetilde{0}\right)^{\mathrm{BCT}}$ is concave with respect to T, K, G, and ϑ_p. □

Data Availability

The data used to support the findings of this study are available from the corresponding author upon request.

Conflicts of Interest

The authors declare that there are no conflicts of interest regarding the publication of this article.

References

[1] European Central Bank, "Supply chain disruptions and the effects on the global economy," 2021, https://www.ecb.europa.eu/pub/economic-bulletin/focus/2022/html/ecb.ebbox202108_01%7Ee8ceebe51f.en.html.

[2] Markets and Markets, "Covid-19 impact on logistics supply chain industry market," 2021, https://www.marketsandmarkets.com/Market-Reports/covid-19-impact-on-logistics-supply-chain-industry-market-244593137.html.

[3] Z. Zhang, D. Guan, R. Wang et al., "Embodied carbon emissions in the supply chains of multinational enterprises," *Nature Climate Change*, vol. 10, no. 12, pp. 1096–1101, 2020.

[4] Brookings, "Tracking emissions by country and sector," 2022, https://www.brookings.edu/blog/future-development/2022/11/29/tracking-emissions-by-country-and-sector/.

[5] United Nations Framework Convention on Climate Change, "Sharm el-sheikh climate change conference-november 2022," 2022, https://unfccc.int/cop27.

[6] J. Sarkis, "Supply chain sustainability: learning from the COVID-19 pandemic," *International Journal of Operations and Production Management*, vol. 41, no. 1, pp. 63–73, 2020.

[7] S. Ruidas, M. R. Seikh, and P. K. Nayak, "A production inventory model with interval-valued carbon emission parameters under price-sensitive demand," *Computers and Industrial Engineering*, vol. 154, Article ID 107154, 2021.

[8] L. Klapper, L. Laeven, and R. Rajan, "Trade credit contracts," *Review of Financial Studies*, vol. 25, no. 3, pp. 838–867, 2012.

[9] J. Lee, B. Bagheri, and H. A. Kao, "A Cyber-Physical Systems architecture for Industry 4.0-based manufacturing systems," *Manufacturing Letters*, vol. 3, pp. 18–23, 2015.

[10] H. Lasi, P. Fettke, H. G. Kemper, T. Feld, and M. Hoffmann, "Industry 4.0," *Business & Information Systems Engineering*, vol. 6, no. 4, pp. 239–242, 2014.

[11] A. Suta and Á Tóth, "Systematic review on blockchain research for sustainability accounting applying methodology coding and text mining," *Cleaner Engineering and Technology*, vol. 14, Article ID 100648, 2023.

[12] S. Das, G. Mandal, F. Akhtar, A. Akbar Shaikh, and A. Kumar Bhunia, "Pricing and dynamic service policy for an imperfect production system: extended Pontryagin's maximum principle for interval control problems," *Expert Systems with Applications*, vol. 238, Article ID 122090, 2024.

[13] M. Al-Salamah, "Economic production quantity in an imperfect manufacturing process with synchronous and asynchronous flexible rework rates," *Operations Research Perspectives*, vol. 6, Article ID 100103, 2019.

[14] F. Lin, T. Jia, R. Y. Fung, and P. Wu, "Impacts of inspection rate on integrated inventory models with defective items considering capacity utilization: rework-versus delivery-priority," *Computers and Industrial Engineering*, vol. 156, Article ID 107245, 2021.

[15] W. A. Jauhari and I. D. Wangsa, "A manufacturer-retailer inventory model with remanufacturing, stochastic demand, and green investments," *Process Integration and Optimization for Sustainability*, vol. 6, no. 2, pp. 253–273, 2022.

[16] H. Ali, S. Das, and A. Akbar Shaikh, "Investigate an imperfect green production system considering rework policy via Teaching-Learning-Based Optimizer algorithm," *Expert Systems with Applications*, vol. 214, Article ID 119143, 2023.

[17] B. K. Dey, A. Datta, and B. Sarkar, "Effectiveness of carbon policies and multi-period delay-in-payments in a global supply chain under remanufacturing consideration," *Journal of Cleaner Production*, vol. 402, Article ID 136539, 2023.

[18] O. Harun, "Alternative shipment policies compared for an international supply chain model with stochastic exchange rate, carbon emission and imperfect quality items," *Sustainable Manufacturing and Service Economics*, vol. 1, Article ID 10002, 2022.

[19] S. Priyan and R. Uthayakumar, "Mathematical modeling and computational algorithm to solve multi-echelon multi-constraint inventory problem with errors in quality inspection," *Journal of Mathematical Modelling and Algorithms in Operations Research*, vol. 14, no. 1, pp. 67–89, 2015.

[20] W. Ahmed, M. Moazzam, B. Sarkar, and S. Ur Rehman, "Synergic effect of reworking for imperfect quality items with the integration of multi-period delay-in-payment and partial backordering in global supply chains," *Engineering*, vol. 7, no. 2, pp. 260–271, 2021.

[21] S. Tiwari, W. Ahmed, and B. Sarkar, "Sustainable ordering policies for non-instantaneous deteriorating items under carbon emission and multi-trade-credit policies," *Journal of Cleaner Production*, vol. 240, Article ID 118183, 2019.

[22] A. K. Mondal, S. Pareek, K. Chaudhuri, A. Bera, R. Bachar, and B. Sarkar, "Technology license sharing strategy for remanufacturing industries under a closed loop supply chain management bonding," *RAIRO-Operations Research*, vol. 56, no. 4, pp. 3017–3045, 2022.

[23] S. V. Padiyar, N. Bhagat, S. R. Singh, and B. Sarkar, "Joint replenishment strategy for deteriorating multi-item through multi-echelon supply chain model with imperfect production under imprecise and inflationary environment," *RAIRO-Operations Research*, vol. 56, no. 4, pp. 3071–3096, 2022.

[24] M. Mittal and B. Sarkar, "Stochastic behaviour of exchange rate on an international supply chain under random energy price," *Mathematics and Computers in Simulation*, vol. 205, pp. 261–284, 2023.

[25] F. Lin, Y. Shi, and X. Zhuo, "Optimizing order policy and credit term for items with inventory-level-dependent demand under trade credit limit," *Journal of Management Science and Engineering*, vol. 8, no. 4, pp. 413–429, 2023.

[26] J. Kaushik, "An inventory model with permissible delay in payment and different interest rate charges," *Decision Analytics Journal*, vol. 6, Article ID 100180, 2023.

[27] M. Kumari, P. Kanti De, P. Narang, and N. H. Shah, "Integrated optimization of inventory, replenishment, and vehicle routing for a sustainable supply chain utilizing a novel hybrid algorithm with carbon emission regulation," *Expert Systems with Applications*, vol. 220, Article ID 119667, 2023.

[28] A. H. M. Mashud, S. Miah, Y. Daryanto, R. K. Chakrabortty, S. M. Hasan, and M.-L. Tseng, "Inventory decisions on the transportation system and carbon emissions under COVID-19 effects: a sensitivity analysis," *Computers & Industrial Engineering*, vol. 171, Article ID 108393, 2022.

[29] A. Priyamvada and A. Kumar, "Modelling retail inventory pricing policies under service level and promotional efforts during COVID-19," *Journal of Cleaner Production*, vol. 381, no. 2022, Article ID 134784, 2022.

[30] J. Valizadeh, S. Boloukifar, S. Soltani et al., "Designing an optimization model for the vaccine supply chain during the COVID-19 pandemic," *Expert Systems with Applications*, vol. 214, Article ID 119009, 2023.

[31] A. H. M. Mashud, M. R. Hasan, Y. Daryanto, and H.-M. Wee, "A resilient hybrid payment supply chain inventory model for post Covid-19 recovery," *Computers and Industrial Engineering*, vol. 157, Article ID 107249, 2021.

[32] M. Alkahtani, M. Omair, Q. S. Khalid, G. Hussain, I. Ahmad, and C. Pruncu, "A COVID-19 supply chain management strategy based on variable production under uncertain environment conditions," *International Journal of Environmental Research and Public Health*, vol. 18, no. 4, p. 1662, 2021.

[33] D. Das, G. C. Samanta, A. Barman, P. K. De, and K. K. Mohanta, "A recovery mathematical model for the impact of supply chain interruptions during the lockdown in COVID-19 using two warehouse perishable inventory policies," *Results in Control and Optimization*, vol. 9, Article ID 100184, 2022.

[34] W. Xie and H. Tian, "The effect of the COVID-19 pandemic on corporate trade credit financing," *Economics Letters*, vol. 232, Article ID 111339, 2023.

[35] S. Priyan, R. Udayakumar, P. Mala, M. Prabha, and A. Ghosh, "A sustainable dual-channel inventory model with trapezoidal fuzzy demand and energy consumption," *Cleaner Engineering and Technology*, vol. 6, Article ID 100400, 2022.

[36] C.-J. Lu, M. Gu, T.-S. Lee, and C.-T. Yang, "Impact of carbon emission policy combinations on the optimal production-inventory decisions for deteriorating items," *Expert Systems with Applications*, vol. 201, Article ID 117234, 2022.

[37] J. Asadkhani, A. Fallahi, and H. Mokhtari, "A sustainable supply chain under VMI-CS agreement with withdrawal policies for imperfect items," *Journal of Cleaner Production*, vol. 376, Article ID 134098, 2022.

[38] W. A. Jauhari, I. N. Pujawan, M. Suef, and K. Govindan, "Low carbon inventory model for vendor–buyer system with hybrid production and adjustable production rate under stochastic demand," *Applied Mathematical Modelling*, vol. 108, pp. 840–868, 2022.

[39] K. Halat, A. Hafezalkotob, and M. K. Sayadi, "Cooperative inventory games in multi-echelon supply chains under carbon tax policy: vertical or horizontal?" *Applied Mathematical Modelling*, vol. 99, pp. 166–203, 2021.

[40] N. Ahmad, I. Sangal, K. Sharma et al., "A green realistic inventory model with preservation technology for deteriorating items under carbon emission," *Materials Today: Proceedings*, 2023.

[41] Y.-S. Huang, C.-C. Fang, and Y.-A. Lin, "Inventory management in supply chains with consideration of Logistics, green investment, and different carbon emissions policies," *Computers and Industrial Engineering*, vol. 139, Article ID 106207, 2020.

[42] S. Priyan, P. Mala, and M. Palanivel, "A cleaner EPQ inventory model involving synchronous and asynchronous rework process with green technology investment," *Cleaner Logistics and Supply Chain*, vol. 4, Article ID 100056, 2022.

[43] W. A. Jauhari, "Sustainable inventory management for a closed-loop supply chain with energy usage, imperfect production, and green investment," *Cleaner Logistics and Supply Chain*, vol. 4, Article ID 100055, 2022.

[44] S. Ruidas, M. R. Seikh, P. K. Nayak, and M.-L. Tseng, "An interval-valued green production inventory model under controllable carbon emissions and green subsidy via particle swarm optimization," *Soft Computing*, vol. 27, no. 14, pp. 9709–9733, 2023.

[45] S. Priyan, "Effect of green investment to reduce carbon emissions in an imperfect production system," *Journal of Climate Finance*, vol. 2, Article ID 100007, 2023.

[46] B. Marchi and S. Zanoni, "Technical note on Inventory management in supply chains with consideration of Logistics, green investment, and different carbon emissions policies," *Computers and Industrial Engineering*, vol. 175, Article ID 108870, 2023.

[47] W. A. Jauhari, S. C. Novia Ramadhany, C. Nur Rosyidi, U. Mishra, and H. Hishamuddin, "Pricing and green inventory decisions for a supply chain system with green investment and carbon tax regulation," *Journal of Cleaner Production*, vol. 425, Article ID 138897, 2023.

[48] W. A. Jauhari, I. D. Wangsa, H. Hishamuddin, and N. Rizky, "A sustainable vendor-buyer inventory model with incentives, green investment and energy usage under stochastic demand," *Cogent Business and Management*, vol. 10, no. 1, Article ID 2158609, 2023.

[49] X. He, "Effects of the green policy environment on renewable energy investment and effect evaluation of green policies," *Discrete Dynamics in Nature and Society*, vol. 2023, Article ID 8698548, 16 pages, 2023.

[50] B. S. O. Alsaedi, O. A. Alamri, M. K. Jayaswal, and M. Mittal, "A sustainable green supply chain model with carbon emissions for defective items under learning in a fuzzy environment," *Mathematics*, vol. 11, no. 2, p. 301, 2023.

[51] W. Jauhari, "Integrated inventory model for three-layer supply chains with stochastic demand," *International Journal of Operational Research*, vol. 13, no. 3, pp. 295–317, 2012.

[52] S. Ruidas, M. R. Seikh, and P. K. Nayak, "An EPQ model with stock and selling price dependent demand and variable production rate in interval environment," *International Journal of System Assurance Engineering and Management*, vol. 11, no. 2, pp. 385–399, 2020.

[53] S. Ruidas, M. R. Seikh, and P. K. Nayak, "Pricing strategy in an interval-valued production inventory model for high-tech products under demand disruption and price revision," *Journal of Industrial and Management Optimization*, vol. 19, no. 9, pp. 6451–6477, 2023.

[54] F. Longo, L. Nicoletti, A. Padovano, G. D'Atri, and M. Forte, "Blockchain-enabled supply chain: an experimental study," *Computers and Industrial Engineering*, vol. 136, pp. 57–69, 2019.

[55] R. Azzi, R. K. Chamoun, and M. Sokhn, "The power of a blockchain-based supply chain," *Computers and Industrial Engineering*, vol. 135, pp. 582–592, 2019.

[56] P. Helo and Y. Hao, "Blockchains in operations and supply chains: a model and reference implementation," *Computers & Industrial Engineering*, vol. 136, pp. 242–251, 2019.

[57] Y. Wei, F. Chen, and H. Wang, "Inventory and production dynamics in a discrete-time vendor-managed inventory supply chain system," *Discrete Dynamics in Nature and Society*, vol. 2018, Article ID 6091946, 15 pages, 2018.

[58] V. K. Manupati, T. Schoenherr, M. Ramkumar, S. M. Wagner, S. K. Pabba, and R. Inder Raj Singh, "A blockchain-based approach for a multi-echelon sustainable supply chain," *International Journal of Production Research*, vol. 58, no. 7, pp. 2222–2241, 2020.

[59] S. Zhu, J. Li, S. Wang, Y. Xia, and Y. Wang, "The role of blockchain technology in the dual-channel supply chain dominated by a brand owner," *International Journal of Production Economics*, vol. 258, Article ID 108791, 2023.

[60] X. Li, "Inventory management and information sharing based on blockchain technology," *Computers and Industrial Engineering*, vol. 179, Article ID 109196, 2023.

[61] X. Xu, P. He, L. Zhou, and T. C. E. Cheng, "Coordination of a platform-based supply chain in the marketplace or reselling mode considering cross-channel effect and blockchain technology," *European Journal of Operational Research*, vol. 309, no. 1, pp. 170–187, 2023.

[62] A. Modares, N. M. Farimani, and F. Dehghanian, "A new vendor-managed inventory model by applying blockchain technology and considering environmental problems," *Process Integration and Optimization for Sustainability*, vol. 7, no. 5, pp. 1211–1239, 2023.

[63] C. Allenbrand, "Smart contract-enabled consortium blockchains for the control of supply chain information distortion," *Block: Research and Applications*, vol. 4, no. 3, Article ID 100134, 2023.

[64] Y. Yu, S. Zhou, and Y. Shi, "Information sharing or not across the supply chain: the role of carbon emission reduction," *Transportation Research Part E: Logistics and Transportation Review*, vol. 137, Article ID 101915, 2020.

[65] X. Vives, *Oligopoly Pricing: Old Ideas and New Tools*, MIT press, Cambridge, MA, USA, 1999.
[66] Carbonbrief, "Uncertainty in climate science," 2021, https://www.carbonbrief.org/uncertainty-in-climate-science/.
[67] B. Niu, Z. Mu, B. Cao, and J. Gao, "Should multinational firms implement blockchain to provide quality verification?" *Transportation Research Part E: Logistics and Transportation Review*, vol. 145, Article ID 102121, 2021.
[68] M. Wang, L. Zhao, and M. Herty, "Modelling carbon trading and refrigerated logistics services within a fresh food supply chain under carbon cap-and-trade regulation," *International Journal of Production Research*, vol. 56, no. 12, pp. 4207–4225, 2018.
[69] V. Babich and G. Hilary, "OM Forum—distributed ledgers and operations: what operations management researchers should know about blockchain technology," *Manufacturing and Service Operations Management*, vol. 22, no. 2, pp. 223–240, 2020.
[70] B. Sarkar and B. Dey, "Is online-to-offline customer care support essential for consumer service?" *Journal of Retailing and Consumer Services*, vol. 75, Article ID 103474, 2023.